SANDIA REPORT

2005-2895
Unlimited Release
Printed April 2005 (revised Jan. 2006)

Domain Decomposition Methods for Advection Dominated Linear–Quadratic Elliptic Optimal Control Problems

Roscoe A. Bartlett (SNL), Matthias Heinkenschloss (Rice University),
Denis Ridzal, (Rice University), Bart G. van Bloemen Waanders (SNL)

Prepared by
Sandia National Laboratories
Albuquerque, New Mexico 87185 and Livermore, California 94550

Sandia is a multiprogram laboratory operated by Sandia Corporation,
a Lockheed Martin Company, for the United States Department of Energy's
National Nuclear Security Administration under Contract DE-AC04-94-AL85000.

Issued by Sandia National Laboratories, operated for the United States Department of Energy by Sandia Corporation.

Available to DOE and DOE contractors from
U.S. Department of Energy
Office of Scientific and Technical Information
P.O. Box 62
Oak Ridge, TN 37831

Telephone:	(865) 576-8401
Facsimile:	(865) 576-5728
E-Mail:	reports@adonis.osti.gov
Online ordering:	http://www.doe.gov/bridge

Available to the public from
U.S. Department of Commerce
National Technical Information Service
5285 Port Royal Rd
Springfield, VA 22161

Telephone:	(800) 553-6847
Facsimile:	(703) 605-6900
E-Mail:	orders@ntis.fedworld.gov
Online ordering:	http://www.ntis.gov/ordering.htm

2005-2895
Unlimited Release
Printed April 2005 (revised Jan. 2006)

Domain Decomposition Methods for Advection Dominated Linear–Quadratic Elliptic Optimal Control Problems

Roscoe A. Bartlett
Optimization/Uncertainty Est Dept (9211)
Sandia National Laboratories, MS 0370
P.O. Box 5800
Albuquerque, NM 87185-0370

Matthias Heinkenschloss
Department of Computational and Applied Mathematics
MS-134
Rice University
6100 Main Street
Houston, TX 77005-1892

Denis Ridzal
Department of Computational and Applied Mathematics
MS-134
Rice University
6100 Main Street
Houston, TX 77005-1892

Bart G. van Bloemen Waanders
Optimization/Uncertainty Est Dept (9211)
Sandia National Laboratories, MS 0370
P.O. Box 5800
Albuquerque, NM 87185-0370

Abstract

We present an optimization-level domain decomposition (DD) preconditioner for the solution of advection dominated elliptic linear–quadratic optimal control problems. The DD preconditioner is based on a decomposition of the optimality conditions for the elliptic linear–quadratic optimal control problem into smaller subdomain optimality conditions with Dirichlet boundary conditions for the states and the adjoints on the subdomain interfaces. These subdomain optimality conditions are coupled through Robin transmission conditions for the states and the adjoints. The parameters in the Robin transmission condition depend on the advection. This decomposition leads to a Schur complement system in which the unknowns are the state and adjoint variables on the subdomain interfaces. The Schur complement operator is the sum of subdomain Schur complement operators, the application of which is shown to correspond to the solution of subdomain optimal control problems, which are essentially smaller copies of the original optimal control problem. We show that, under suitable conditions, the application of the inverse of the subdomain Schur complement operators requires the solution of a subdomain elliptic linear–quadratic optimal control problem with Robin boundary conditions for the state.

Numerical tests for problems with distributed and with boundary control show that the dependence of the preconditioners on mesh size and subdomain size is comparable to its counterpart applied to a single advection dominated equation. These tests also show that the preconditioners are insensitive to the size of the control regularization parameter.

Acknowledgment

The work of Matthias Heinkenschloss and Denis Ridzal was supported in part by NSF grants ACI-0121360, CNS–0435425 and Sandia National Laboratories CSRF-284340.

The format of this report is based on information found in [29].

Contents

Figures

Tables

Domain Decomposition Methods for Advection Dominated Linear–Quadratic Elliptic Optimal Control Problems

1 Introduction

Optimization problems governed by (systems of) advection dominated elliptic partial differential equations (PDEs) arise in many science and engineering applications, see, e.g., [1, 2, 15, 16, 17, 22, 36, 41], either directly or as subproblems in Newton-type or sequential quadratic optimization algorithms for the solution of optimization problems governed by (systems of) nonlinear PDEs. This paper is concerned with optimization–level domain decomposition preconditioners for such problems. We focus our presentation on the linear quadratic optimal control problem

$$\text{minimize } \frac{1}{2}\int_\Omega (y(x)-\widehat{y}(x))^2 dx + \frac{\alpha}{2}\int_\Omega u^2(x)dx \tag{1.1}$$

subject to

$$-\varepsilon\Delta y(x) + \mathbf{a}(x)\cdot\nabla y(x) + r(x)y(x) = f(x)+u(x), \qquad x\in\Omega, \tag{1.2a}$$

$$y(x) = 0, \qquad x\in\partial\Omega_D, \tag{1.2b}$$

$$\varepsilon\frac{\partial}{\partial\mathbf{n}}y(x) = g(x), \qquad x\in\partial\Omega_N, \tag{1.2c}$$

where $\partial\Omega_D, \partial\Omega_N$ are boundary segments with $\partial\Omega_D = \partial\Omega\setminus\partial\Omega_N$, $\mathbf{a}, f, g, r, \widehat{y}$ are given functions, $\varepsilon, \alpha > 0$ are given scalars, and $\mathbf{n}$ denotes the outward unit normal. Assumptions on these data that ensure the well-posedness of the problem will be given in the next section. The material presented in this paper can be extended to boundary control problems and several other objective functionals. The problem (1.1), (1.2) is an optimization problem in the unknowns y and u, referred to as the state and the control, respectively.

Our domain decomposition method for the solution of (1.1), (1.2) generalizes the Neumann-Neumann domain decomposition method, which is well known for the solution of single PDEs (see, e.g., the books [32, 38, 39]) to the optimization context. Optimization–level Neumann-Neumann domain decomposition methods for elliptic optimal control problems were first introduced in [19, 20] for problems without advection. However, the presence of strong advection can significantly alter the behavior of solution algorithms and typically requires their modification. For domain decomposition methods applied to single advection dominated PDEs a nice overview of this issue is given in [39, Sec. 11.5.1]. The aim of our paper is to tackle this issue for optimal control problems.

The domain decomposition methods presented in this paper are formulated at the optimization level. The domain Ω is partitioned into non-overlapping subdomains. Our domain

decomposition methods decompose the optimality conditions for (1.1), (1.2). Auxiliary state and so-called adjoints (Lagrange multipliers) are introduced at the subdomain interfaces. The states, adjoints, and controls in the interior of the subdomains are then viewed as implicit functions of the states and adjoints on the interface, defined through the solution of subdomain optimality conditions. To obtain a solution of the original problem (1.1), (1.2), the states and adjoints on the interface have to be chosen such that the implicitly defined states, adjoints, and controls in the interior of the subdomains satisfy certain Robin transmission conditions at the interface boundaries. These transmission conditions take into account the advection dominated nature of the state equation and are motivated by [3, 4].

The optimization-level domain decomposition described in the previous paragraph leads to a Schur complement formulation for the optimality system. The application of the Schur complement to a given vector of states and adjoints on the interface, requires the parallel solution of subdomain optimal control problems that are essentially copies of (1.1), (1.2) restricted to the subdomains, but with Dirichlet boundary conditions at the subdomain interfaces. The Schur complement is the sum of subdomain Schur complements. Each subdomain Schur complement is shown to be invertible. The application of the inverse of each subdomain Schur complement requires the solution of another subdomain optimal control problem that is also essentially a copy of (1.1), (1.2) restricted to the respective subdomain, but with Robin boundary conditions at the subdomain interfaces. The inverses of the subdomain Schur complements are used to derive preconditioners for the Schur complement.

Section 2 briefly reviews results on the existence, uniqueness and characterization of solutions of (1.1), (1.2). The domain decomposition, interface conditions, subdomain Schur complements and their inverses are discussed in Section 3 using a variational point of view. The corresponding algebraic form, properties of the subdomain Schur complement matrices and some implementation details are presented in Section 4. The performance of the preconditioners on some model problems with distributed control and boundary control are documented in Section 5.

Throughout this paper we use the following notation for norms and inner products. Let $G \subset \Omega \subset \mathbb{R}^d$ or $G \subset \partial\Omega$. We define $\langle f, g\rangle_G = \int_G f(x)g(x)dx$, $\|v\|^2_{0,G} = \int_G v^2(x)dx$, $|v|^2_{1,G} = \int_G \nabla v(x) \cdot \nabla v(x)dx$, and $\|v\|^2_{1,G} = \|v\|^2_{0,G} + |v|^2_{1,G}$. If $G = \Omega$ we omit G and simply write $\langle f, g\rangle$, etc.

2 The Model Problem

Multiplication of the advection diffusion equation (1.2) by a test function

$$\phi \in Y \stackrel{\text{def}}{=} \left\{\phi \in H^1(\Omega) : \phi = 0 \text{ on } \partial\Omega_D\right\},$$

integration over Ω, and performing integration by parts leads to the following weak form

$$a(y,\phi) + b(u,\phi) = \langle f, \phi\rangle + \langle g, \phi\rangle_{\partial\Omega_N} \quad \forall \phi \in Y, \tag{2.1}$$

where

$$a(y,\phi) = \int_\Omega \varepsilon \nabla y(x)\cdot\nabla\phi(x) + \mathbf{a}(x)\cdot\nabla y(x)\phi(x) + r(x)y(x)\phi(x)dx, \tag{2.2a}$$

$$b(u,\phi) = -\int_\Omega u(x)\phi(x)dx, \tag{2.2b}$$

$$\langle f,\phi\rangle = \int_\Omega f(x)\phi(x)dx, \qquad \langle g,\phi\rangle_{\partial\Omega_N} = \int_{\partial\Omega_N} g(x)\phi(x)dx. \tag{2.2c}$$

We assume that

$$f \in L^2(\Omega), \mathbf{a} \in \left(W^{1,\infty}(\Omega)\right)^2, r \in L^\infty(\Omega), g \in L^2(\partial\Omega_N), \varepsilon > 0, \tag{2.3a}$$

$$\partial\Omega_N \subset \{x \in \partial\Omega : \ \mathbf{a}(x)\cdot\mathbf{n}(x) \geq 0\} \tag{2.3b}$$

and

$$r(x) - \tfrac{1}{2}\nabla\cdot\mathbf{a}(x) \geq r_0 > 0 \text{ a.e. in } \Omega. \tag{2.3c}$$

If $\partial\Omega_D$ has a nonempty relative interior, then (2.3c) can be replaced by

$$r(x) - \tfrac{1}{2}\nabla\cdot\mathbf{a}(x) \geq r_0 \geq 0 \text{ a.e. in } \Omega. \tag{2.3d}$$

Since

$$\begin{aligned} a(y,\phi) = &\int_\Omega \varepsilon\nabla y(x)\cdot\nabla\phi(x) + \tfrac{1}{2}\mathbf{a}(x)\cdot\nabla y(x)\phi(x) - \tfrac{1}{2}\mathbf{a}(x)\cdot\nabla\phi(x)y(x) \\ &+(r(x) - \tfrac{1}{2}\nabla\cdot\mathbf{a}(x))y(x)\phi(x)dx + \int_{\Omega_N}\tfrac{1}{2}\mathbf{a}(x)\cdot\mathbf{n}\, y(x)\phi(x)dx, \end{aligned} \tag{2.4}$$

the assumptions (2.3), guarantee that the bilinear form a is continuous on $Y\times Y$ and Y-elliptic (e.g., [31, p. 165], [34, Sec III.1], or [30, Sec. 2.5]).

We are interested in the solution of the optimal control problem

$$\text{minimize} \quad \frac{1}{2}\|y-\widehat{y}\|_0^2 + \frac{\alpha}{2}\|u\|_0^2, \tag{2.5a}$$

$$\text{subject to} \quad a(y,\phi) + b(u,\phi) = \langle f,\phi\rangle + \langle g,\phi\rangle_{\partial\Omega_N} \quad \forall\phi\in Y, \tag{2.5b}$$
$$y \in Y, u \in U,$$

where the control space is given by $U = L^2(\Omega)$ and the state space Y is as specified above.

As we have stated before, the bilinear form a is continuous on $Y\times Y$ and Y-elliptic under the assumptions (2.3). Hence the theory in [28, Sec. II.1] guarantees the existence of a unique solution $(y,u)\in Y\times U$ of (2.5).

Theorem 2.1 *If* (2.3) *are satisfied, the optimal control problem* (2.5) *has a unique solution* $(y,u)\in Y\times U$.

The theory in [28, Sec. II.1] also provides necessary and sufficient optimality conditions, which can be best described using the Lagrangian

$$L(y,u,p) = \frac{1}{2}\|y-\widehat{y}\|_0^2 + \frac{\alpha}{2}\|u\|_0^2 + a(y,p) + b(u,p) - \langle f,p\rangle - \langle g,p\rangle_{\partial\Omega_N}. \tag{2.6}$$

The necessary and, for our model problem, sufficient optimality conditions can be obtained by setting the partial Fréchet-derivatives of (2.6) with respect to states $y \in Y$, controls $u \in U$ and adjoints $p \in Y$ equal to zero. This gives the following system consisting of the adjoint equation

$$a(\psi,p) = -\langle y-\hat{y},\psi\rangle \quad \forall \psi \in Y, \tag{2.7a}$$

the gradient equation

$$b(w,p) + \alpha\langle u,w\rangle = 0 \quad \forall w \in U, \tag{2.7b}$$

and the state equation

$$a(y,\phi) + b(u,\phi) = \langle f,\phi\rangle + \langle g,\phi\rangle_{\partial\Omega_N} \quad \forall \phi \in Y. \tag{2.7c}$$

The gradient equation (2.7b) simply means that

$$p(x) = \alpha u(x) \qquad x \in \Omega \tag{2.8}$$

and (2.7a) is the weak form of

$$-\varepsilon\Delta p(x) - \mathbf{a}(x)\cdot\nabla p(x) + (r(x) - \nabla\cdot\mathbf{a}(x))p(x) = -(y(x)-\hat{y}(x)), \quad x \in \Omega, \tag{2.9a}$$

$$p(x) = 0, \quad x \in \partial\Omega_D, \tag{2.9b}$$

$$\varepsilon\frac{\partial}{\partial\mathbf{n}}p(x) + \mathbf{a}(x)\cdot\mathbf{n}(x)\; p(x) = 0, \quad x \in \partial\Omega_N. \tag{2.9c}$$

After finite element discretization, the optimal control problem (2.5) leads to a large-scale linear quadratic optimization problem. It is well known that application of the standard linear finite element method to advection–diffusion equations (1.2) leads to computed solutions with large spurious oscillations, unless the mesh size is sufficiently small relative to the Péclet number (e.g., [31, Sec. 8], [34], or [30]). To allow relatively coarse meshes, we use the streamline upwind/Petrov–Galerkin (SUPG) method [7]. We mention that if the SUPG method, or other stabilized finite element methods are used, the optimality system of the linear quadratic optimization problem corresponding to the discretization of the optimal control problem (2.5) is in general no longer equal to the discretization of the optimality system (2.7). The differences are due to the stabilization term. For a more detailed treatment, we refer to [1, 8]. The papers [1, 8] show that for linear finite elements and suitable choice of the stabilization parameter, these differences are small. In our numerical solution of the problem, we discretize the optimal control problem (2.5) using the SUPG method.

3 Domain Decomposition Schur Complement Formulation of the Example Problem

3.1 Discretization of the Example Problem

We discretize (2.5) using conforming linear finite elements. Let $\{T_l\}$ be a triangulation of Ω and let $\{x_j\}$ be the set of vertices in the triangulation. We divide Ω into nonoverlapping subdomains Ω_i, $i = 1,\ldots,s$, such that each T_l belongs to exactly one $\overline{\Omega}_i$. We define

$$\Gamma_i = \partial\Omega_i \setminus \partial\Omega$$

and

$$\Gamma = \cup_{i=1}^{s} \Gamma_i.$$

The unit outward normal of Ω_i is denoted by $\mathbf{n}_i$. The state y is approximated using piecewise linear functions. We define the finite dimensional state space

$$Y^h = \left\{ \phi_h \in H^1(\Omega) : \ \phi_h = 0 \text{ on } \partial\Omega_D, \ \phi_h|_{T_l} \in P^1(T_l) \text{ for all } l \right\}.$$

To formulate our domain decomposition approach we also define

$$\begin{aligned}
Y_i^h &= \left\{ \phi_h \in H^1(\Omega_i) : \ \phi_h = 0 \text{ on } \partial\Omega_i \cap \partial\Omega_D, \ \phi_h|_{T_l} \in P^1(T_l) \text{ for all } T_l \subset \overline{\Omega}_i \right\}, && i = 1,\ldots,s, \\
Y_{i,0}^h &= \left\{ \phi_h \in Y_i^h : \ \phi_h = 0 \text{ on } \Gamma_i \right\}, && i = 1,\ldots,s, \\
Y_{i,\Gamma_i}^h &= \left\{ \phi_h \in Y_i^h : \ \phi_h(x_j) = 0, x_j \in \Omega_i \cup (\partial\Omega_i \cap \partial\Omega) \right\}, && i = 1,\ldots,s,
\end{aligned} \tag{3.1}$$

and

$$Y_\Gamma^h = \left\{ \phi_h \in Y^h : \ \phi_h(x_j) = 0, x_j \in \cup_{i=1}^{s} \Omega_i \cup \partial\Omega \right\}.$$

We identify $(\phi_h)_i \in Y_{i,0}^h$ with a function in Y^h by extending $(\phi_h)_i \in Y_{i,0}^h$ by zero onto Ω. Hence, the state space can be decomposed into

$$Y^h = Y_\Gamma^h \oplus_{i=1}^{s} Y_{i,0}^h.$$

For our discretization of the control we use piecewise linear functions in Ω. However, our discretization of the control is somewhat nonstandard. A straightforward discretization of the control space by piecewise linear functions would lead to

$$U^h = \left\{ u_h \in C^0(\Omega) : \ u \in P^1(T_l) \text{ for all } T_l \subset \overline{\Omega} \right\}. \tag{3.2}$$

A domain decomposition formulation based on such a discretization would introduce 'interface controls' (dotted hat function in the left plot in Figure 3.1) defined on a 'band' of width $O(h)$ around $\partial\Omega_i \cap \partial\Omega_j$, $i \neq j$. See the left plot in Figure 3.1. Since the evaluation of $u \in L^2(\Omega)$ on $\partial\Omega_i \cap \partial\Omega_j$ does not make sense, we avoid interface controls.

We discretize the control u by a function which is continuous on each Ω_i, $i = 1,\dots,s$, and linear on each $\Omega_i \cap T_l$. The discretized control is not assumed to be continuous on $\partial\Omega_i \cap \partial\Omega_j$, $i \neq j$. In particular, for each point $x_k \in \partial\Omega_i \cap \partial\Omega_j$, $i \neq j$, there are two discrete controls u_{k_i}, u_{k_j} belonging to subdomains Ω_i and Ω_j, respectively (see the right plot in Figure 3.1). Since the control space is $L^2(\Omega)$, this is a legitimate discretization. We define the discrete control spaces

$$U_i^h = \left\{ u_h \in C^0(\Omega_i) \,:\, u_h \in P^1(T_l) \text{ for all } T_l \subset \overline{\Omega}_i \right\}. \tag{3.3}$$

We identify U_i^h with a subspace of $L^2(\Omega)$ by extending functions $u_i \in U_i^h$ by zero onto Ω. We define

$$U^h = \cup_{i=1}^s U_i^h \subset L^2(\Omega).$$

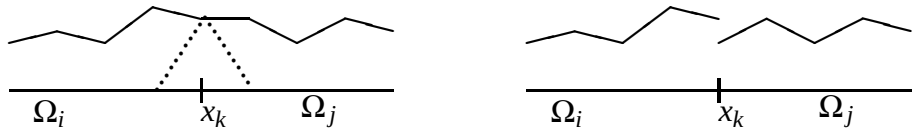

Figure 3.1. Sketch of the control discretization for $\Omega \subset \mathbb{R}$

For advection dominated problems the standard Galerkin method applied to the state equation (2.1) produces strongly oscillatory approximations, unless the mesh size h is chosen sufficiently small relative to $\varepsilon/\|\mathbf{a}\|_{0,\infty}$. To obtain approximate solutions of better quality on coarser meshes, various stabilization techniques have been proposed. For an overview see [31, Secs. 8.3.2,8.4] or [34, Sec.3.2]. We use the streamline upwind/Petrov Galerkin (SUPG) method of Hughes and Brooks [7]. The SUPG method computes an approximation $y_h \in Y^h$ of the solution y of the state equation (2.5b) by solving

$$a_h(y_h,\phi_h) + b_h(u_h,\phi_h) = \langle f,\phi_h\rangle_h + \langle g,\phi_h\rangle_{\partial\Omega_N} \quad \forall \phi_h \in Y^h, \tag{3.4}$$

where

$$\begin{aligned}
a_h(y_h,\phi_h) &= a(y_h,\phi_h) + \sum_{T_e\in\overline{\Omega}} \tau_e \langle -\varepsilon\Delta y_h + \mathbf{a}\cdot\nabla y_h + r y_h, \mathbf{a}\cdot\nabla\phi_h\rangle_{T_e}, && \text{(3.5a)}\\
b_h(u_h,\phi_h) &= b(u_h,\phi_h) + \sum_{T_e\in\overline{\Omega}} -\tau_e \langle u_h, \mathbf{a}\cdot\nabla\phi_h\rangle_{T_e}, && \text{(3.5b)}\\
\langle f,\phi_h\rangle_h &= \langle f,\phi_h\rangle + \sum_{T_e\in\overline{\Omega}} \tau_e \langle f, \mathbf{a}\cdot\nabla\phi_h\rangle_{T_e}, && \text{(3.5c)}
\end{aligned}$$

and $\tau_e > 0$ is a stabilization parameter that is chosen depending on the mesh size and the problem parameters ε, $\mathbf{a}$ and r.

Our discretization of the optimal control problem (2.5) is given by

$$\begin{aligned} &\text{minimize} && \frac{1}{2}\|y_h - \widehat{y}\|_0^2 + \frac{\alpha}{2}\|u_h\|_0^2, && \text{(3.6a)}\\ &\text{subject to} && a_h(y_h,\phi_h) + b_h(u_h,\phi_h) = \langle f,\phi_h\rangle_h + \langle g,\phi_h\rangle_{\partial\Omega_N} \quad \forall \phi_h \in Y^h, && \text{(3.6b)}\\ & && y_h \in Y^h, u_h \in U^h. \end{aligned}$$

The necessary and sufficient optimality conditions for (3.6) are given by

$$\begin{aligned} a_h(\psi_h,p_h) + \langle y_h,\psi_h\rangle &= \langle \hat{y},\psi_h\rangle && \forall \psi_h \in Y^h, && \text{(3.7a)}\\ \alpha\langle u_h,\mu_h\rangle + b_h(\mu_h,p_h) &= 0 && \forall \mu_h \in U^h, && \text{(3.7b)}\\ a_h(y_h,\phi_h) + b_h(u_h,\phi_h) &= \langle f,\phi_h\rangle_h + \langle g,\phi_h\rangle_{\Gamma_n} && \forall \phi_h \in Y^h. && \text{(3.7c)} \end{aligned}$$

The system (3.7) may also be viewed as a discretization of (2.7). However, as we have discussed already at the end of Section 2, the discretization of the system (2.7) of optimality conditions using SUPG will lead to a slightly different system than (3.7). Everything that follows can be easily applied to the SUPG discretization of the system (2.7) of optimality conditions.

3.2 Domain Decomposition of the Example Problem

To decompose the discrete optimality conditions (3.7), we need local bilinear forms corresponding to the subdomains Ω_i. For advection dominated problems, this requires some care. See, e.g., [39, Sec.11.5.1] for an overview. The straight forward restriction of a defined in (2.2a) to the subdomain Ω_i is given by

$$\widetilde{a}_i(y_h,\phi_h) = \int_{\Omega_i} \varepsilon\nabla y_h(x)\cdot\nabla\phi_h(x) + \mathbf{a}(x)\cdot\nabla y_h(x)\phi_h(x) + r(x)y_h(x)\phi_h(x)dx. \qquad (3.8)$$

Integration by parts and application of the chain rule to $\nabla\cdot(\mathbf{a}(x)\phi_h(x))$ show that

$$\begin{aligned} \widetilde{a}_i(y_h,\phi_h) \;=\; & \int_{\Omega_i} \varepsilon\nabla y_h(x)\cdot\nabla\phi_h(x) + \tfrac{1}{2}\mathbf{a}(x)\cdot\nabla y_h(x)\phi_h(x)\\ & \quad -\tfrac{1}{2}\mathbf{a}(x)\cdot\nabla\phi_h(x)y_h(x) + (r(x) - \tfrac{1}{2}\nabla\cdot\mathbf{a}(x))y_h(x)\phi_h(x)dx\\ & + \tfrac{1}{2}\int_{\partial\Omega_i\cap\partial\Omega_N} \mathbf{a}(x)\cdot\mathbf{n}_i y_h(x)\phi_h(x)dx + \tfrac{1}{2}\int_{\partial\Omega_i\setminus\partial\Omega} \mathbf{a}(x)\cdot\mathbf{n}_i y_h(x)\phi_h(x)dx \end{aligned}$$

for all $y_h, \phi_h \in Y_i^h$. Because of the last boundary integral, the assumptions (2.3) no longer guarantee that a_i is Y_i^h–elliptic. Hence, we follow [4] and use the local bilinear form

$$\begin{aligned} a_i(y_h,\phi_h) &= \widetilde{a}_i(y_h,\phi_h) - \tfrac{1}{2}\int_{\partial\Omega_i\setminus\partial\Omega} \mathbf{a}(x)\cdot\mathbf{n}_i y_h(x)\phi_h(x)dx \qquad (3.9)\\ &= \int_{\Omega_i} \varepsilon\nabla y_h(x)\cdot\nabla\phi_h(x) + \tfrac{1}{2}\mathbf{a}(x)\cdot\nabla y_h(x)\phi_h(x)\\ &\qquad -\tfrac{1}{2}\mathbf{a}(x)\cdot\nabla\phi_h(x)y_h(x) + (r(x)-\tfrac{1}{2}\nabla\cdot\mathbf{a}(x))y_h(x)\phi_h(x)dx\\ &\quad +\tfrac{1}{2}\int_{\partial\Omega_i\cap\partial\Omega_N}\mathbf{a}(x)\cdot\mathbf{n}_i y_h(x)\phi_h(x)dx. \end{aligned}$$

Note that

$$\sum_{i=1}^{s}\tfrac{1}{2}\int_{\partial\Omega_i\setminus\partial\Omega}\mathbf{a}(x)\cdot\mathbf{n}_i y_h(x)\phi_h(x)dx = \sum_{i=1}^{s}\sum_{j\neq i}\tfrac{1}{2}\int_{\partial\Omega_i\cap\partial\Omega_j}\mathbf{a}(x)\cdot\mathbf{n}_i y_h(x)\phi_h(x)dx = 0$$

since each boundary integral $\int_{\partial\Omega_i\cap\partial\Omega_j}$ appears twice in the summation, once with integrand $\mathbf{a}(x)\cdot\mathbf{n}_i y_h(x)\phi_h(x)$, the other time with integrand $\mathbf{a}(x)\cdot\mathbf{n}_j y_h(x)\phi_h(x) = -\mathbf{a}(x)\cdot\mathbf{n}_i y_h(x)\phi_h(x)$. Hence

$$\sum_{i=1}^{s} a_i(y_h,\phi_h) = \sum_{i=1}^{s}\widetilde{a}_i(y_h,\phi_h) = a(y_h,\phi_h) \quad \forall y_h,\phi_h\in Y_i^h,$$

i.e., the global problem is not altered.

Accounting for the SUPG terms, we define

$$\begin{aligned} a_{i,h}(y_h,\phi_h) &= \widetilde{a}_i(y_h,\psi_h) - \tfrac{1}{2}\int_{\partial\Omega_i\setminus\partial\Omega_N}\mathbf{a}(x)\cdot\mathbf{n}_i y_h(x)\phi_h(x)dx\\ &\quad + \sum_{T_e\in\overline{\Omega_i}}\tau_e\langle -\varepsilon\Delta y_h + \mathbf{a}\cdot\nabla y_h + r y_h, \mathbf{a}\cdot\nabla\phi_h\rangle_{T_e}, \qquad (3.10a)\\ b_{i,h}(u_h,\phi_h) &= -\langle u_h,\phi_h\rangle_{\Omega_i} + \sum_{T_e\in\overline{\Omega_i}} -\tau_e\langle u_h,\mathbf{a}\cdot\nabla\phi_h\rangle_{T_e}, \qquad (3.10b)\\ \langle f,\phi_h\rangle_{\Omega_i,h} &= \langle f,\phi_h\rangle_{\Omega_i} + \sum_{T_e\in\overline{\Omega_i}}\tau_e\langle f,\mathbf{a}\cdot\nabla\phi_h\rangle_{T_e}. \qquad (3.10c) \end{aligned}$$

Now, we decompose the optimality system (3.7) by introducing artificial state and adjoint variables $y_\Gamma, p_\Gamma \in Y_\Gamma^h$ on the subdomain interfaces. Given $y_\Gamma, p_\Gamma \in Y_\Gamma^h$ we consider

$$\begin{aligned} a_{i,h}(\psi_i,p_i) + \langle y_i,\psi_i\rangle_{\Omega_i} &= \langle\hat{y},\psi_i\rangle_{\Omega_i} && \forall\psi_i\in Y_{i,0}^h, && (3.11a)\\ b_{i,h}(\mu_i,p_i) + \langle u_i,\mu_i\rangle_{\Omega_i} &= 0 && \forall\mu_i\in U_i^h, && (3.11b)\\ a_{i,h}(y_i,\phi_i) + b_{i,h}(u_i,\phi_i) &= \langle f,\phi_i\rangle_{\Omega_i,h} + \langle g,\phi_i\rangle_{\partial\Omega_i\cap\partial\Omega_N} && \forall\phi_i\in Y_{i,0}^h, && (3.11c)\\ y_i = y_\Gamma,\quad p_i &= p_\Gamma && \text{on } \Gamma_i, && (3.11d) \end{aligned}$$

and

$$\begin{aligned}
&\sum_{i=1}^{s} a_{i,h}(y_i, \mathcal{R}_h^{\mathrm{a}}(v_\Gamma, q_\Gamma)) + b_{i,h}(u_i, \mathcal{R}_h^{\mathrm{a}}(v_\Gamma, q_\Gamma)) \\
&\qquad + a_{i,h}(\mathcal{R}_h^{\mathrm{s}}(v_\Gamma, q_\Gamma), p_i) + \langle y_i, \mathcal{R}_h^{\mathrm{s}}(v_\Gamma, q_\Gamma)\rangle_{\Omega_i} \\
= \;& \sum_{i=1}^{s} \langle f, \mathcal{R}_h^{\mathrm{a}}(v_\Gamma, q_\Gamma)\rangle_{\Omega_i,h} + \langle g, \mathcal{R}_h^{\mathrm{a}}(v_\Gamma, q_\Gamma)\rangle_{\partial\Omega_i \cap \partial\Omega_N} + \langle \hat{y}_i, \mathcal{R}_h^{\mathrm{s}}(v_\Gamma, q_\Gamma)\rangle_{\Omega_i}
\end{aligned} \tag{3.12}$$

for all $v_\Gamma, q_\Gamma \in Y_\Gamma^h$, where

$$\mathcal{R}_h^{\mathrm{s}}, \mathcal{R}_h^{\mathrm{a}} : Y_\Gamma^h \times Y_\Gamma^h \to Y^h \tag{3.13a}$$

are continuous linear extension operators with

$$\mathcal{R}_h^{\mathrm{s}}(v_\Gamma, q_\Gamma)(x) = v_\Gamma(x), \quad \mathcal{R}_h^{\mathrm{a}}(v_\Gamma, q_\Gamma)(x) = q_\Gamma(x), \tag{3.13b}$$

for all $x \in \Gamma$ and for all $v_\Gamma, q_\Gamma \in Y_\Gamma^h$.

Theorem 3.1 *If $(y,u,p) \in Y^h \times U^h \times Y^h$ solves* (3.7)*, then $y_i = y|_{\Omega_i}$, $u_i = u|_{\Omega_i}$, $p_i = p|_{\Omega_i}$, $i = 1,\ldots,s$, solve* (3.11)*,* (3.12)*.*

If $(y_\Gamma, p_\Gamma) \in Y_\Gamma^h \times Y_\Gamma^h$ is such that the solution $(y_i,u_i,p_i) \in Y_i^h \times U_i^h \times Y_i^h$, of (3.11)*, $i = 1,\ldots,s$, satisfies the interface conditions* (3.12)*, then $(y,u,p) \in Y^h \times U^h \times Y^h$ given by $y|_{\Omega_i} = y_i$, $u|_{\Omega_i} = u_i$, $p|_{\Omega_i} = p_i$, $i = 1,\ldots,s$, solves* (3.7)*.*

The proof of this result is analogous to the proof of [32, Lemma 1.2.1] and is omitted.

We will view the solution of (3.11) as an affine linear function of (y_Γ, p_Γ) and then consider (3.12) as a linear equation in (y_Γ, p_Γ). We will describe this process using the variational formulation in Subsection 3.3 and we will describe the algebraic version in Section 4. The latter is used computationally. Section 4 can be read without knowledge of the material in the remainder of this section. The main purpose of the remainder of this section is to connect the subproblems that need to be solved to the original optimal control problem (1.1).

We close this subsection with an interpretation of (3.11) and (3.12). We note that any continuous linear extensions with (3.13b) can be admitted. One choice would be to define $\mathcal{R}_h^{\mathrm{s}}(v_\Gamma, q_\Gamma)$ as the extension of v_Γ onto Ω and $\mathcal{R}_h^{\mathrm{a}}(v_\Gamma, q_\Gamma)$ as the extension of q_Γ onto Ω. However, the Schur complement formulation, which perhaps is most easily introduced from the matrix point of view (see Section 4), corresponds to different extension operators. These will be introduced in Section 3.3.

Remark 3.2 *i. The systems* (3.11)*, $i = 1,\dots,s$, can be interpreted as the finite element discretization of*

$$
\begin{aligned}
-\varepsilon\Delta y_i(x) + \mathbf{a}(x)\cdot\nabla y_i(x) + r(x)y_i(x) &= f(x) + u_i(x) && \text{in } \Omega_i, && (3.14a)\\
y_i(x) &= 0 && \text{on } \partial\Omega_i \cap \partial\Omega_D, && (3.14b)\\
\varepsilon\frac{\partial}{\partial \mathbf{n}} y_i(x) &= g(x) && \text{on } \partial\Omega_i \cap \partial\Omega_N, && (3.14c)\\
y_i(x) &= y_\Gamma(x) && \text{on } \Gamma_i, && (3.14d)\\
-\varepsilon\Delta p_i(x) - \mathbf{a}(x)\cdot\nabla p_i(x) & \\
+(r(x) - \nabla\cdot\mathbf{a}(x))p_i(x) &= -(y_i(x) - \hat{y}(x)) && \text{in } \Omega_i, && (3.14e)\\
p_i(x) &= 0, && \text{on } \partial\Omega_i \cap \partial\Omega_D, && (3.14f)\\
\varepsilon\frac{\partial}{\partial \mathbf{n}} p_i(x) + \mathbf{a}(x)\cdot\mathbf{n}(x)\; p_i(x) &= 0 && \text{on } \partial\Omega_i \cap \partial\Omega_N, && (3.14g)\\
p_i(x) &= p_\Gamma(x) && \text{on } \Gamma_i, && (3.14h)\\
\alpha u_i(x) - p_i(x) &= 0 && \text{on } \partial\Omega \cap \partial\Omega_i. && (3.14i)
\end{aligned}
$$

ii. Applying the arguments in [20] to the advection diffusion case, the system (3.14) *may be viewed as the necessary and sufficient optimality conditions for*

$$
\text{minimize } \tfrac{1}{2}\int_{\Omega_i} (y_i(x) - \hat{y}(x))^2 dx + \frac{\alpha}{2}\int_{\Omega_i} u_i^2(x)dx + \int_{\Gamma_i} \varepsilon\frac{\partial}{\partial \mathbf{n}_i} y_i(x) p_\Gamma(x) dx, \qquad (3.15a)
$$

subject to

$$
\begin{aligned}
-\varepsilon\Delta y_i(x) + \mathbf{a}(x)\cdot\nabla y_i(x) + r(x)y_i(x) &= f(x) + u_i(x) && \text{in } \Omega_i, && (3.15b)\\
y_i(x) &= 0 && \text{on } \partial\Omega_i \cap \partial\Omega_D, && (3.15c)\\
\varepsilon\frac{\partial}{\partial \mathbf{n}} y_i(x) &= g(x) && \text{on } \partial\Omega_i \cap \partial\Omega_N, && (3.15d)\\
y_i(x) &= y_\Gamma(x) && \text{on } \Gamma_i, && (3.15e)
\end{aligned}
$$

Note that since $y_i(x) = y_\Gamma(x)$ on Γ_i is given, the objective function (3.15a) *can be replaced by*

$$
\tfrac{1}{2}\int_{\Omega_i} (y_i(x) - \hat{y}(x))^2 dx + \frac{\alpha}{2}\int_{\Omega_i} u_i^2(x)dx + \int_{\Gamma_i} \left(\varepsilon\frac{\partial}{\partial \mathbf{n}_i} - \tfrac{1}{2}\mathbf{a}(x)\mathbf{n}_i\right) y_i(x) p_\Gamma(x) dx.
$$

The addition of $\int_{\Gamma_i} -\frac{1}{2}\mathbf{a}(x)\mathbf{n}_i y_i(x) p_\Gamma(x)dx = \int_{\Gamma_i} -\frac{1}{2}\mathbf{a}(x)\mathbf{n}_i y_\Gamma(x) p_\Gamma(x)dx$ only shifts the objective function by a constant, but does not change the solution y_i, u_i, p_i of (3.15)*. The latter form of the objective function emphasizes the connection with the transmission conditions* (3.12) *which will be discussed next.*

iii. The interface condition (3.12) *can be interpreted as*

$$
\begin{aligned}
\left(\varepsilon\tfrac{\partial}{\partial \mathbf{n}_i} - \tfrac{1}{2}\mathbf{a}(x)\mathbf{n}_i\right) y_i(x) &= -\left(\varepsilon\tfrac{\partial}{\partial \mathbf{n}_j} - \tfrac{1}{2}\mathbf{a}(x)\mathbf{n}_j\right) y_j(x) \quad x \in \partial\Omega_i \cap \partial\Omega_j,\\
\left(\varepsilon\tfrac{\partial}{\partial \mathbf{n}_i} + \tfrac{1}{2}\mathbf{a}(x)\mathbf{n}_i\right) p_i(x) &= -\left(\varepsilon\tfrac{\partial}{\partial \mathbf{n}_j} + \tfrac{1}{2}\mathbf{a}(x)\mathbf{n}_j\right) p_j(x) \quad x \in \partial\Omega_i \cap \partial\Omega_j,
\end{aligned} \qquad (3.16)
$$

for $i,j=1,\dots,s$, $i\neq j$. In fact, let $\phi=\mathcal{R}_h^{\mathrm{a}}(v_\Gamma,q_\Gamma)+\sum_{i=1}^s\phi_i$, $\psi=\mathcal{R}_h^{\mathrm{s}}(v_\Gamma,q_\Gamma)+\sum_{i=1}^s\psi_i$. Equations (3.11), *$i=1,\dots,s$, and* (3.12) *imply*

$$\begin{aligned}&\sum_{i=1}^s a_{i,h}(y_i,\phi)+b_{i,h}(u_i,\phi)+a_{i,h}(\psi,p_i)+\langle y_i,\psi\rangle_{\Omega_i}\\ =\;&\sum_{i=1}^s\langle f,\phi\rangle_{\Omega_i,h}+\langle g,\phi\rangle_{\partial\Omega_i\cap\partial\Omega_N}+\langle\hat{y}_i,\psi\rangle_{\Omega_i}\quad\forall\phi,\psi\in Y^h.\end{aligned}\tag{3.17}$$

If we insert (3.10) *without the SUPG terms,* (3.17) *yields*

$$\begin{aligned}0=&\sum_{i=1}^s\int_{\Omega_i}\varepsilon\nabla y_i(x)\cdot\nabla\phi(x)+\mathbf{a}(x)\cdot\nabla y_i(x)\phi(x)+r(x)y_i(x)\phi(x)dx\\&-\tfrac{1}{2}\int_{\partial\Omega_i\setminus\partial\Omega}\mathbf{a}(x)\cdot\mathbf{n}_i y_i(x)\phi(x)dx-\int_{\Omega_i}f(x)\phi(x)-u_i(x)\phi(x)dx-\int_{\partial\Omega_i\cap\partial\Omega_N}g(x)\phi(x)dx,\\0=&\sum_{i=1}^s\int_{\Omega_i}\varepsilon\nabla\psi(x)\cdot\nabla p_i(x)+\mathbf{a}(x)\cdot\nabla\psi(x)p_i(x)+r(x)\psi(x)p_i(x)dx\\&-\tfrac{1}{2}\int_{\partial\Omega_i\setminus\partial\Omega}\mathbf{a}(x)\cdot\mathbf{n}_i\,p_i(x)\psi(x)dx+\int_{\Omega_i}(\widehat{y}(x)-y_i(x))\psi(x)dx\end{aligned}$$

for all $\phi,\psi\in Y^h$. Integration by parts finally leads to

$$\begin{aligned}0=&\sum_{i=1}^s\int_{\Omega_i}(-\varepsilon\Delta y_i(x)+\mathbf{a}(x)\cdot\nabla y_i(x)+r(x)y_i(x)-f(x)-u_i(x))\phi(x)dx\\&+\int_{\partial\Omega_i\setminus\partial\Omega}(\varepsilon\frac{\partial}{\partial\mathbf{n}_i}-\tfrac{1}{2}\mathbf{a}(x)\cdot\mathbf{n}_i)y_i(x)\phi(x)dx+\int_{\partial\Omega_i\cap\partial\Omega_N}(\varepsilon\frac{\partial}{\partial\mathbf{n}_i}y_i(x)-g(x))\phi(x)dx,\end{aligned}\tag{3.18a}$$

$$\begin{aligned}0=&\sum_{i=1}^s\int_{\Omega_i}(-\varepsilon\Delta p_i(x)-\mathbf{a}(x)\cdot\nabla p_i(x)+(r(x)-\nabla\cdot\mathbf{a}(x))p_i(x)+\widehat{y}(x)-y_i(x))\psi(x)dx\\&+\int_{\partial\Omega_i\setminus\partial\Omega}(\varepsilon\frac{\partial}{\partial\mathbf{n}_i}+\tfrac{1}{2}\mathbf{a}(x)\cdot\mathbf{n}_i)p_i(x)\psi(x)dx+\int_{\partial\Omega_i\cap\partial\Omega_N}\varepsilon\frac{\partial}{\partial\mathbf{n}_i}p_i(x)\psi(x)dx\end{aligned}\tag{3.18b}$$

for all $\phi,\psi\in Y^h$. Since y_i,u_i,p_i satisfy (3.14)*, equations* (3.18) *reduce to*

$$\begin{aligned}0=&\sum_{i=1}^s\int_{\partial\Omega_i\setminus\partial\Omega}(\varepsilon\frac{\partial}{\partial\mathbf{n}_i}-\tfrac{1}{2}\mathbf{a}(x)\cdot\mathbf{n}_i)y_i(x)\phi(x)dx&&\forall\phi\in Y^h,\\0=&\sum_{i=1}^s\int_{\partial\Omega_i\setminus\partial\Omega}(\varepsilon\frac{\partial}{\partial\mathbf{n}_i}+\tfrac{1}{2}\mathbf{a}(x)\cdot\mathbf{n}_i)p_i(x)\psi(x)dx&&\forall\psi\in Y^h.\end{aligned}$$

This leads to (3.16)*.*

Remark 3.3 *We briefly comment on the subproblems that would arise if we had used the unmodified local bilinear forms $a_{i,h}(y_h,\phi_h)=\widetilde{a}_i(y_h,\psi_h)$ instead of* (3.10)*.*

i. If $a_{i,h}(y_h,\phi_h)=\widetilde{a}_i(y_h,\psi_h)$*, the systems* (3.11)*,* $i=1,\ldots,s$*, can still be interpreted as the finite element discretization of* (3.14) *which, in turn, can be viewed as the optimality conditions for* (3.15)*.*

iii. If $a_{i,h}(y_h,\phi_h)=\widetilde{a}_i(y_h,\psi_h)$*, the interface condition* (3.12) *can be interpreted as*

$$\begin{array}{rcll} \varepsilon\frac{\partial}{\partial \mathbf{n}_i}y_i(x) & = & -\varepsilon\frac{\partial}{\partial \mathbf{n}_j}y_j(x) & x\in\partial\Omega_i\cap\partial\Omega_j, \\ \left(\varepsilon\frac{\partial}{\partial \mathbf{n}_i}+\mathbf{a}(x)\mathbf{n}_i\right)p_i(x) & = & -\left(\varepsilon\frac{\partial}{\partial \mathbf{n}_j}+\mathbf{a}(x)\mathbf{n}_j\right)p_j(x) & x\in\partial\Omega_i\cap\partial\Omega_j, \end{array} \tag{3.19}$$

for $i,j=1,\ldots,s$*,* $i\neq j$*.*

3.3 Schur Complement Formulation

As we have stated earlier, we will view the solution of (3.11) as an affine linear function of (y_Γ,p_Γ) and then consider (3.12) as a linear equation in (y_Γ,p_Γ). The variational formulation of this process is studied here. It complements Section 4, but is not required for the reading of Section 4.

For $i=1,\ldots,s$, we define the linear operators

$$\mathcal{H}_i^h : Y_\Gamma^h\times Y_\Gamma^h \to Y_i^h\times U_i^h\times Y_i^h \tag{3.20a}$$

with

$$\mathcal{H}_i^h(y_\Gamma,p_\Gamma)=\begin{pmatrix}(\mathcal{H}_i^h)^y(y_\Gamma,p_\Gamma)\\(\mathcal{H}_i^h)^u(y_\Gamma,p_\Gamma)\\(\mathcal{H}_i^h)^p(y_\Gamma,p_\Gamma)\end{pmatrix}=\begin{pmatrix}y_i^0\\u_i^0\\p_i^0\end{pmatrix}, \tag{3.20b}$$

where (y_i^0,u_i^0,p_i^0) is the solution of (3.11) with $f=0$, $g=0$ and $\hat{y}=0$.

Let $\langle\!\langle\cdot,\cdot\rangle\!\rangle$ denote the duality pairing between $(Y_\Gamma^h)^2$ and $((Y_\Gamma^h)^*)^2$. We define the linear subdomain Schur complement operator

$$\mathcal{S}_i^h : (Y_\Gamma^h)^2 \to ((Y_\Gamma^h)^*)^2, \tag{3.21a}$$

$i=1,\ldots,s$, with

$$\begin{aligned} &\langle\!\langle \mathcal{S}_i^h(y_\Gamma,p_\Gamma),(v_\Gamma,q_\Gamma)\rangle\!\rangle \\ &\quad= a_{i,h}((\mathcal{H}_i^h)^y(y_\Gamma,p_\Gamma),(\mathcal{H}_i^h)^p(v_\Gamma,q_\Gamma))+b_{i,h}((\mathcal{H}_i^h)^u(y_\Gamma,p_\Gamma),(\mathcal{H}_i^h)^p(v_\Gamma,q_\Gamma)) \\ &\qquad+a_{i,h}((\mathcal{H}_i^h)^y(v_\Gamma,q_\Gamma),(\mathcal{H}_i^h)^p(y_\Gamma,p_\Gamma)) \\ &\qquad+\langle(\mathcal{H}_i^h)^y(y_\Gamma,p_\Gamma),(\mathcal{H}_i^h)^y(v_\Gamma,q_\Gamma)\rangle_{\Omega_i}. \end{aligned} \tag{3.21b}$$

The definition of $\mathcal{H}_i^h$ implies that

$$\alpha\langle(\mathcal{H}_i^h)^u(y_\Gamma,p_\Gamma),\mu_i\rangle_{\Omega_i}+b_{i,h}(\mu_i,(\mathcal{H}_i^h)^p(y_\Gamma,p_\Gamma))=0\quad\forall\mu_i\in U_i^h$$

(cf., (3.11b)) and, hence, we can write

$$\begin{aligned}
&\langle\!\langle \mathcal{S}_i^h(y_\Gamma,p_\Gamma),(v_\Gamma,q_\Gamma)\rangle\!\rangle \\
&\quad = a_{i,h}((\mathcal{H}_i^h)^y(y_\Gamma,p_\Gamma),(\mathcal{H}_i^h)^p(v_\Gamma,q_\Gamma)) + b_{i,h}((\mathcal{H}_i^h)^u(y_\Gamma,p_\Gamma),(\mathcal{H}_i^h)^p(v_\Gamma,q_\Gamma)) \\
&\qquad + b_{i,h}((\mathcal{H}_i^h)^u(v_\Gamma,q_\Gamma),(\mathcal{H}_i^h)^p(y_\Gamma,p_\Gamma)) + \alpha\langle(\mathcal{H}_i^h)^u(y_\Gamma,p_\Gamma),(\mathcal{H}_i^h)^u(v_\Gamma,q_\Gamma)\rangle_{\Omega_i} \\
&\qquad + a_{i,h}((\mathcal{H}_i^h)^y(v_\Gamma,q_\Gamma),(\mathcal{H}_i^h)^p(y_\Gamma,p_\Gamma)) \\
&\qquad + \langle(\mathcal{H}_i^h)^y(y_\Gamma,p_\Gamma),(\mathcal{H}_i^h)^y(v_\Gamma,q_\Gamma)\rangle_{\Omega_i}. \qquad (3.21c)
\end{aligned}$$

We define $r_i \in ((Y_\Gamma^h)^*)^2$, $i = 1,\ldots,s$, as

$$\begin{aligned}
&\langle\!\langle r_i,(v_\Gamma,q_\Gamma)\rangle\!\rangle \\
&\quad = \langle f,(\mathcal{H}_i^h)^p(v_\Gamma,q_\Gamma)\rangle_{\Omega_i,h} + \langle g,(\mathcal{H}_i^h)^p(v_\Gamma,q_\Gamma)\rangle_{\partial\Omega_i\cap\partial\Omega_N} + \langle \hat{y}_i,(\mathcal{H}_i^h)^y(v_\Gamma,q_\Gamma)\rangle_{\Omega_i} \\
&\qquad - a_{i,h}(y_i,(\mathcal{H}_i^h)^p(v_\Gamma,q_\Gamma)) - b_{i,h}(u_i,(\mathcal{H}_i^h)^p(v_\Gamma,q_\Gamma)) \\
&\qquad - a_{i,h}((\mathcal{H}_i^h)^y(v_\Gamma,q_\Gamma),p_i) - \langle y_i,(\mathcal{H}_i^h)^y(v_\Gamma,q_\Gamma)\rangle_{\Omega_i}, \qquad (3.22)
\end{aligned}$$

where (y_i,u_i,p_i) is the solution of (3.11) with $y_\Gamma = 0$ and $p_\Gamma = 0$.

Theorem 3.1 with $\mathcal{R}_h^{\mathrm{s}}(v_\Gamma,q_\Gamma)|_{\Omega_i} = (\mathcal{H}_i^h)^y(v_\Gamma,q_\Gamma)$ and $\mathcal{R}_h^{\mathrm{a}}(v_\Gamma,q_\Gamma)|_{\Omega_i} = (\mathcal{H}_i^h)^p(v_\Gamma,q_\Gamma)$ implies that the system (3.7) of optimality conditions is equivalent to the Schur complement system

$$\sum_{i=1}^s \mathcal{S}_i^h(y_\Gamma,p_\Gamma) = \sum_{i=1}^s r_i \quad \text{in } ((Y_\Gamma^h)^*)^2. \qquad (3.23)$$

The next result establishes the invertibility of the subdomain Schur complement operator $\mathcal{S}_i$.

Theorem 3.4 *Let $r_i = (r_i^y, r_i^p) \in ((Y_{i,\Gamma_i}^h)^*)^2$.*

i. If (2.3a)–(2.3c) *hold and if the stabilization parameter τ_e is sufficiently small, then the unique solution $(y_\Gamma,p_\Gamma) \in (Y_{i,\Gamma_i}^h)^2$ of*

$$\mathcal{S}_i(y_\Gamma,p_\Gamma) = r_i \qquad (3.24)$$

is given by

$$y_\Gamma = y_i|_{\Gamma_i}, \quad p_\Gamma = p_i|_{\Gamma_i},$$

where $(y_i,u_i,p_i) \in Y_i^h \times U_i^h \times Y_i^h$ is the unique solution of

$$a_{i,h}(\psi,p_i) + \langle y_i,\psi\rangle_{\Omega_i} = \langle r_i^y,\psi\rangle_{\Gamma_i} \qquad \forall \psi \in Y_i^h, \qquad (3.25a)$$

$$b_{i,h}(\mu,p_i) + \alpha\langle u_i,\mu\rangle_{\Omega_i} = 0 \qquad \forall \mu \in U_i^h, \qquad (3.25b)$$

$$a_{i,h}(y_i,\psi) + b_{i,h}(u_i,\psi) = \langle r_i^p,\psi\rangle_{\Gamma_i} \qquad \forall \psi \in Y_i^h. \qquad (3.25c)$$

ii. If the relative interior of $\partial\Omega_i \cap \partial\Omega_D$ is nonempty, then the assumption (2.3c) *in part i. can be replaced by* (2.3d).

The proof of this theorem is very similar to its counterpart in [20]. The inclusion of the advection as well as the SUPG stabilization, however, require a few subtle modifications. For completeness, we include the poof.

Proof: By definition (3.21) of $\mathcal{S}_i$, the equality (3.24) can be written as

$$\begin{aligned} & a_{i,h}((\mathcal{H}_i^h)^y(y_\Gamma,p_\Gamma),(\mathcal{H}_i^h)^p(v_\Gamma,q_\Gamma)) + b_{i,h}((\mathcal{H}_i^h)^u(y_\Gamma,p_\Gamma),(\mathcal{H}_i^h)^p(v_\Gamma,q_\Gamma)) \\ & + a_{i,h}((\mathcal{H}_i^h)^y(v_\Gamma,q_\Gamma),(\mathcal{H}_i^h)^p(y_\Gamma,p_\Gamma)) + \langle(\mathcal{H}_i^h)^y(y_\Gamma,p_\Gamma),(\mathcal{H}_i^h)^y(v_\Gamma,q_\Gamma)\rangle_{\Omega_i} \\ = \;& \langle r_i^y, v_\Gamma\rangle_{\Gamma_i} + \langle r_i^p, q_\Gamma\rangle_{\Gamma_i} \end{aligned} \tag{3.26}$$

for all $v_\Gamma, q_\Gamma \in Y_{i,\Gamma_i}^h$. Using the definition (3.20) of $\mathcal{H}_i(y_\Gamma,p_\Gamma)$ together with (3.26), we see that (3.24) is equivalent to

$$\begin{aligned} & a_{i,h}((\mathcal{H}_i^h)^y(y_\Gamma,p_\Gamma),(\mathcal{H}_i^h)^p(v_\Gamma,q_\Gamma)) \\ & + b_{i,h}((\mathcal{H}_i^h)^u(y_\Gamma,p_\Gamma),(\mathcal{H}_i^h)^p(v_\Gamma,q_\Gamma)) \\ & + a_{i,h}((\mathcal{H}_i^h)^y(v_\Gamma,q_\Gamma),(\mathcal{H}_i^h)^p(y_\Gamma,p_\Gamma)) \\ & + \langle(\mathcal{H}_i^h)^y(y_\Gamma,p_\Gamma),(\mathcal{H}_i^h)^y(v_\Gamma,q_\Gamma)\rangle_{\Omega_i} = \langle r_i^y, v_\Gamma\rangle_{\Gamma_i} + \langle r_i^p, q_\Gamma\rangle_{\Gamma_i} \quad \forall v_\Gamma, q_\Gamma \in Y_{i,\Gamma_i}^h, \end{aligned} \tag{3.27a}$$

$$a_{i,h}(\psi^0,p_i) + \langle y_i,\psi^0\rangle_{\Omega_i} = 0 \qquad \forall \psi^0 \in Y_{i,0}^h, \tag{3.27b}$$

$$b_{i,h}(\mu,p_i) + \alpha\langle u_i,\mu\rangle_{\Omega_i} = 0 \qquad \forall \mu \in U_i^h, \tag{3.27c}$$

$$a_{i,h}(y_i,\phi^0) + b_{i,h}(u_i,\phi^0) = 0 \qquad \forall \phi^0 \in Y_{i,0}^h, \tag{3.27d}$$

$$y_i = y_\Gamma, \quad p_i = p_\Gamma \qquad \text{on } \Gamma, \tag{3.27e}$$

If we set $\psi = \psi^0 + (\mathcal{H}_i^h)^y(y_\Gamma,p_\Gamma) \in Y_i^h$ and $\phi = \phi^0 + (\mathcal{H}_i^h)^p(y_\Gamma,p_\Gamma) \in Y_i^h$, then (3.27) is equivalent to

$$a_{i,h}(\psi,p_i) + \langle y_i,\psi\rangle_{\Omega_i} = \langle r_i^y,\psi\rangle_{\Gamma_i}, \qquad \forall \psi \in Y_i^h, \tag{3.28a}$$

$$b_{i,h}(\mu,p_i) + \alpha\langle u_i,\mu\rangle_{\Omega_i} = 0 \qquad \forall \mu \in U_i^h, \tag{3.28b}$$

$$a_{i,h}(y_i,\phi) + b_{i,h}(u_i,\phi) = \langle r_i^p,\phi\rangle_{\Gamma_i} \qquad \forall \phi \in Y_i^h, \tag{3.28c}$$

$$y_i = y_\Gamma, \quad p_i = p_\Gamma \qquad \text{on } \Gamma, \tag{3.28d}$$

The assertion follows if we prove that (3.25) has a unique solution $(y_i,u_i,p_i) \in Y_i^h \times U_i^h \times Y_i^h$. Let $(y_i^1,u_i^1,p_i^1),(y_i^2,u_i^2,p_i^2) \in Y_i^h \times U_i^h \times Y_i^h$ be solutions of (3.25). Then $(e_i^y,e_i^u,e_i^p) = (y_i^1-y_i^2,u_i^1-u_i^2,p_i^1-p_i^2) \in Y_i^h \times U_i^h \times Y_i^h$ satisfies

$$a_{i,h}(\psi,e_i^p) + \langle e_i^y,\psi\rangle_{\Omega_i} = 0 \qquad \forall \psi \in Y_i^h, \tag{3.29a}$$

$$b_{i,h}(\mu,e_i^p) + \alpha\langle e_i^u,\mu\rangle_{\Omega_i} = 0 \qquad \forall \mu \in U_i^h, \tag{3.29b}$$

$$a_{i,h}(e_i^y,\phi) + b_{i,h}(e_i^u,\phi) = 0 \qquad \forall \phi \in Y_i^h. \tag{3.29c}$$

If we set $\psi = e_i^y$, $\mu = e_i^u$, and $\phi = -e_i^p$ in (3.29) and add the resulting equations, we obtain

$$0 = \|e_i^y\|_{0,\Omega_i}^2 + \alpha\|e_i^u\|_{0,\Omega_i}^2.$$

Hence $e_i^y = 0$ and $e_i^u = 0$. Now, consider (3.29a) with $\psi = e_i^p$. Using the definitions (3.9) and (3.10) and the assumptions (2.3a), (2.3b), (2.3d) we have

$$\begin{aligned} 0 = a_{i,h}(e_i^p, e_i^p) &= \int_{\Omega_i} \varepsilon \nabla e_i^p(x) \cdot \nabla e_i^p(x) + (r(x) - \tfrac{1}{2}\nabla \cdot \mathbf{a}(x))(e_i^p(x))^2 dx \\ &\quad + \tfrac{1}{2} \int_{\partial\Omega_i \cap \partial\Omega_N} \mathbf{a}(x) \cdot \mathbf{n}_i \, (e_i^p(x))^2 dx, \\ &\quad + \sum_{T_e \in \overline{\Omega_i}} \tau_e \langle -\varepsilon \Delta e_i^p + \mathbf{a} \cdot \nabla e_i^p + r e_i^p, \mathbf{a} \cdot \nabla e_i^p \rangle_{T_e} \\ &\geq \varepsilon |\nabla e_i^p|_{1,\Omega_i} + r_0 \|e_i^p\|_{0,\Omega_i} \\ &\quad + \sum_{T_e \in \overline{\Omega_i}} \tau_e \langle -\varepsilon \Delta e_i^p + \mathbf{a} \cdot \nabla e_i^p + r e_i^p, \mathbf{a} \cdot \nabla e_i^p \rangle_{T_e}. \end{aligned}$$

(Note that the modification of the local bilinear from (3.9) was used to derive the previous inequality.) Standard SUPG estimates (cf. [25, p. 378] or [34, L. 3.28,p. 231]) show that

$$0 = a_{i,h}(e_i^p, e_i^p) \geq \frac{\varepsilon}{2} |\nabla e_i^p|_{1,\Omega_i} + \frac{r_0}{2} \|e_i^p\|_{0,\Omega_i} + \frac{1}{2} \sum_{T_e \in \overline{\Omega_i}} \tau_e \|\mathbf{a} \cdot \nabla e_i^p\|_{0,T_e},$$

for sufficiently small τ_e. This implies $e_i^p = 0$.

ii. By the same arguments as those applied in part i., we can show $e_i^y = 0$ and $e_i^u = 0$. By a Poincaré inequality, we have $\|e_i^p\|_{0,\Omega_i} \leq c |\nabla e_i^p|_{1,\Omega_i}$. Hence we can modify the estimates above to show that

$$\begin{aligned} 0 &= a_{i,h}(e_i^p, e_i^p) \\ &\geq \varepsilon |\nabla e_i^p|_{1,\Omega_i} + \sum_{T_e \in \overline{\Omega_i}} \tau_e \langle -\varepsilon \Delta e_i^p + \mathbf{a} \cdot \nabla e_i^p + r e_i^p, \mathbf{a} \cdot \nabla e_i^p \rangle_{T_e}, \\ &\geq \frac{\varepsilon}{2} |\nabla e_i^p|_{1,\Omega_i} + \frac{\varepsilon}{2c} \|e_i^p\|_{0,\Omega_i} + \sum_{T_e \in \overline{\Omega_i}} \tau_e \langle -\varepsilon \Delta e_i^p + \mathbf{a} \cdot \nabla e_i^p + r e_i^p, \mathbf{a} \cdot \nabla e_i^p \rangle_{T_e} \\ &\geq \frac{\varepsilon}{4} |\nabla e_i^p|_{1,\Omega_i} + \frac{\varepsilon}{4c} \|e_i^p\|_{0,\Omega_i} + \frac{1}{2} \sum_{T_e \in \overline{\Omega_i}} \tau_e \|\mathbf{a} \cdot \nabla e_i^p\|_{0,T_e} \end{aligned}$$

for sufficiently small τ_e. This implies $e_i^p = 0$. □

Remark 3.5 *i. Equations* (3.25) *can be interpreted as the weak form of*

$$
\begin{aligned}
-\varepsilon\Delta y_i(x) + \mathbf{a}(x)\cdot\nabla y_i(x) + r(x)y_i(x) &= u_i(x) && \text{in } \Omega_i, && \text{(3.30a)}\\
y_i(x) &= 0 && \text{on } \partial\Omega_i\cap\partial\Omega_D, && \text{(3.30b)}\\
\varepsilon\frac{\partial}{\partial\mathbf{n}_i}y_i(x) &= 0 && \text{on } \partial\Omega_i\cap\partial\Omega_N, && \text{(3.30c)}\\
\left(\varepsilon\frac{\partial}{\partial\mathbf{n}_i} - \tfrac{1}{2}\mathbf{a}(x)\cdot\mathbf{n}_i\right)y_i(x) &= r_i^y(x) && \text{on } \Gamma_i, && \text{(3.30d)}\\
-\varepsilon\Delta p_i(x) - \mathbf{a}(x)\cdot\nabla p_i(x) + (r(x) - \nabla\cdot\mathbf{a}(x))p_i(x) &= -y_i(x) && \text{in } \Omega_i, && \text{(3.30e)}\\
p_i(x) &= 0, && \text{on } \partial\Omega_i\cap\partial\Omega_D, && \text{(3.30f)}\\
\varepsilon\frac{\partial}{\partial\mathbf{n}_i}p_i(x) + \mathbf{a}(x)\cdot\mathbf{n}(x)\ p_i(x) &= 0 && \text{on } \partial\Omega_i\cap\partial\Omega_N, && \text{(3.30g)}\\
\left(\varepsilon\frac{\partial}{\partial\mathbf{n}_i} + \tfrac{1}{2}\mathbf{a}(x)\cdot\mathbf{n}_i\right)p_i(x) &= r_i^p(x) && \text{on } \Gamma_i, && \text{(3.30h)}\\
\alpha u_i(x) - p_i(x) &= 0 && \text{on } \partial\Omega\cap\partial\Omega_i. && \text{(3.30i)}
\end{aligned}
$$

The terms $\frac{1}{2}\mathbf{a}(x)\cdot\mathbf{n}_i$ *in (3.30d,h) arise because of the modification* (3.9) *in the local bilinear form* $a_{i,h}$.

ii. The system (3.30) *may be viewed as the necessary and sufficient optimality conditions for*

$$
\text{minimize } \tfrac{1}{2}\int_{\Omega_i} y_i^2(x)dx + \frac{\alpha}{2}\int_{\Omega_i} u_i^2(x)dx - \int_{\Gamma_i} y_i(x)r_i^p(x)dx, \qquad \text{(3.31a)}
$$

subject to

$$
\begin{aligned}
-\varepsilon\Delta y_i(x) + \mathbf{a}(x)\cdot\nabla y_i(x) + r(x)y_i(x) &= u_i(x) && \text{in } \Omega_i, && \text{(3.31b)}\\
y_i(x) &= 0 && \text{on } \partial\Omega_i\cap\partial\Omega_D, && \text{(3.31c)}\\
\varepsilon\frac{\partial}{\partial\mathbf{n}}y_i(x) &= 0, && \text{on } \partial\Omega_i\cap\partial\Omega_N, && \text{(3.31d)}\\
\left(\varepsilon\frac{\partial}{\partial\mathbf{n}_i} - \tfrac{1}{2}\mathbf{a}(x)\cdot\mathbf{n}_i\right)y_i(x) &= r_i^y(x) && \text{on } \Gamma_i, && \text{(3.31e)}
\end{aligned}
$$

Remark 3.6 *If the unmodified local bilinear forms* $a_{i,h}(y_h,\phi_h) = \widetilde{a}_i(y_h,\psi_h)$ *were used instead of* (3.10)*, the invertibility of* $\mathcal{S}_i$ *can no longer be guaranteed in general.*

However, if $a_{i,h}(y_h,\phi_h) = \widetilde{a}_i(y_h,\psi_h)$*, and if* $\mathcal{S}_i$ *is invertible, then the application of its*

inverse corresponds to

$$
\begin{aligned}
-\varepsilon\Delta y_i(x) + \mathbf{a}(x)\cdot\nabla y_i(x) + r(x)y_i(x) &= u_i(x) && \text{in } \Omega_i, && \text{(3.32a)}\\
y_i(x) &= 0, && \text{on } \partial\Omega_i \cap \partial\Omega_D, && \text{(3.32b)}\\
\varepsilon\frac{\partial}{\partial \mathbf{n}_i} y_i(x) &= 0 && \text{on } \partial\Omega_i \cap \partial\Omega_N, && \text{(3.32c)}\\
\varepsilon\frac{\partial}{\partial \mathbf{n}_i} y_i(x) &= r_i^y(x) && \text{on } \Gamma_i, && \text{(3.32d)}\\
-\varepsilon\Delta p_i(x) - \mathbf{a}(x)\cdot\nabla p_i(x) + (r(x) - \nabla\cdot\mathbf{a}(x))p_i(x) &= -y_i(x) && \text{in } \Omega_i, && \text{(3.32e)}\\
p_i(x) &= 0 && \text{on } \partial\Omega_i \cap \partial\Omega_D, && \text{(3.32f)}\\
\varepsilon\frac{\partial}{\partial \mathbf{n}_i} p_i(x) + \mathbf{a}(x)\cdot\mathbf{n}(x)\ p_i(x) &= 0 && \text{on } \partial\Omega_i \cap \partial\Omega_N, && \text{(3.32g)}\\
\left(\varepsilon\frac{\partial}{\partial \mathbf{n}_i} + \mathbf{a}(x)\cdot\mathbf{n}_i\right) p_i(x) &= r_i^p(x) && \text{on } \Gamma_i, && \text{(3.32h)}\\
\alpha u_i(x) - p_i(x) &= 0 && \text{on } \partial\Omega \cap \partial\Omega_i. && \text{(3.32i)}
\end{aligned}
$$

4 Algebraic Formulation

The discretization of the optimal control problem (3.6) using piecewise linear finite elements with SUPG stabilization leads to a large-scale linear quadratic problem of the form

$$
\begin{aligned}
&\text{minimize } \frac{1}{2}\mathbf{y}^T\mathbf{Q}\mathbf{y} + \mathbf{c}^T\mathbf{y} + \frac{\alpha}{2}\mathbf{u}^T\mathbf{R}\mathbf{u}, && \text{(4.1a)}\\
&\text{subject to } \mathbf{A}\mathbf{y} + \mathbf{B}\mathbf{u} = \mathbf{b}. && \text{(4.1b)}
\end{aligned}
$$

For the model problem, the matrices $\mathbf{Q} \in \mathbb{R}^{m\times m}, \mathbf{R} \in \mathbb{R}^{n\times n}$ are mass matrices and are symmetric positive definite. The stiffness matrix $\mathbf{A} \in \mathbb{R}^{m\times m}$ is non-symmetric, but, under the assumptions (2.3) and with sufficiently small stabilization parameter τ_e (cf. [25, p. 378] or [34, L. 3.28,p. 231]), the matrix obeys $\mathbf{y}^T\mathbf{A}\mathbf{y} > 0$ for all $\mathbf{y} \neq 0$. In particular under these conditions $\mathbf{A}$ is invertible. The necessary and sufficient optimality conditions for (4.1) are given by

$$
\begin{pmatrix} \mathbf{Q} & \mathbf{0} & \mathbf{A}^T \\ \mathbf{0} & \alpha\mathbf{R} & \mathbf{B}^T \\ \mathbf{A} & \mathbf{B} & \mathbf{0} \end{pmatrix} \begin{pmatrix} \mathbf{y} \\ \mathbf{u} \\ \mathbf{p} \end{pmatrix} = \begin{pmatrix} -\mathbf{c} \\ \mathbf{0} \\ \mathbf{b} \end{pmatrix}. \qquad \text{(4.2)}
$$

The system matrix in (4.2) is symmetric indefinite and has $m+n$ positive eigenvalues and m negative eigenvalues [14].

4.1 Domain Decomposition Schur Complement Formulation

We can use the decomposition of Ω to decompose the matrices $\mathbf{A}$, etc. Our notation follows the commonly used in the domain decomposition literature, see, e.g., [32, Sec. 2.3] [38, Sec. 4], [39, Sec. 1.2]. Let $\mathbb{I}_i^y$, $i = 1,\ldots,s$, be the restriction operator which maps from the vector of coefficient unknowns on the interface boundary, $\mathbf{y}_\Gamma$, to only those associated with the boundary of Ω_i, and let

$$\mathbb{I}_i = \begin{pmatrix} \mathbb{I}_i^y & \\ & \mathbb{I}_i^p \end{pmatrix}, \quad \mathbb{I}_i^p = \mathbb{I}_i^y. \tag{4.3}$$

After a suitable reordering of rows and columns, the stiffness matrix can be written as

$$\mathbf{A} = \begin{pmatrix} \mathbf{A}_{II}^1 & & & \mathbf{A}_{I\Gamma}^1 \mathbb{I}_1^y \\ & \ddots & & \vdots \\ & & \mathbf{A}_{II}^s & \mathbf{A}_{I\Gamma}^s \mathbb{I}_s^y \\ (\mathbb{I}_1^y)^T \mathbf{A}_{\Gamma I}^1 & \cdots & (\mathbb{I}_s^y)^T \mathbf{A}_{\Gamma I}^s & \mathbf{A}_{\Gamma\Gamma} \end{pmatrix}. \tag{4.4}$$

$\mathbf{A}_{\Gamma\Gamma} = \sum_{i=1}^s (\mathbb{I}_i^y)^T \mathbf{A}_{\Gamma\Gamma}^i \mathbb{I}_i^y$. Similar decompositions can be introduced for $\mathbf{Q}$ and $\mathbf{c}$, as well as $\mathbf{y}, \mathbf{p}$.

The matrices $\mathbf{B}$ and $\mathbf{R}$ associated with the control can be decomposed analogously. After a suitable reordering of rows and columns, the matrix $\mathbf{B}$ can be written as

$$\mathbf{B} = \begin{pmatrix} \mathbf{B}_{II}^1 & & \\ & \ddots & \\ & & \mathbf{B}_{II}^s \\ (\mathbb{I}_1^y)^T \mathbf{B}_{\Gamma I}^1 & \cdots & (\mathbb{I}_s^y)^T \mathbf{B}_{\Gamma I}^s \end{pmatrix}.$$

Note that due to our control discretization, there are not controls associated with the interface Γ. Consequently, there are no $\mathbf{B}_{I\Gamma}^i, \ldots, \mathbf{B}_{\Gamma\Gamma}^i$. The matrix $\mathbf{R}$ and the vector $\mathbf{u}$ can be decomposed analogously. Note that there is no $\mathbf{u}_\Gamma$.

We can now insert the domain decomposition structure of the matrices $\mathbf{A}, \mathbf{Q}, \mathbf{B}, \mathbf{R}$ into (4.2). After a symmetric permutation, (4.2) can be written as

$$\begin{pmatrix} \mathbf{K}_{II}^1 & & & (\mathbf{K}_{\Gamma I}^1)^T \mathbb{I}_1 \\ & \ddots & & \vdots \\ & & \mathbf{K}_{II}^s & (\mathbf{K}_{\Gamma I}^s)^T \mathbb{I}_s \\ \mathbb{I}_1^T \mathbf{K}_{\Gamma I}^1 & \cdots & \mathbb{I}_s^T \mathbf{K}_{\Gamma I}^s & \mathbf{K}_{\Gamma\Gamma} \end{pmatrix} \begin{pmatrix} \mathbf{x}_I^1 \\ \vdots \\ \mathbf{x}_I^d \\ \mathbf{x}_\Gamma \end{pmatrix} = \begin{pmatrix} \mathbf{g}_I^1 \\ \vdots \\ \mathbf{g}_I^d \\ \mathbf{g}_\Gamma \end{pmatrix}, \tag{4.5}$$

where

$$\mathbf{K}_{\Gamma\Gamma}^i = \begin{pmatrix} \mathbf{Q}_{\Gamma\Gamma}^i & (\mathbf{A}_{\Gamma\Gamma}^i)^T \\ \mathbf{A}_{\Gamma\Gamma}^i & \end{pmatrix}, i = 1,\ldots,s, \quad \mathbf{K}_{\Gamma\Gamma} = \sum_{i=1}^s \mathbb{I}_i^T \mathbf{K}_{\Gamma\Gamma}^i \mathbb{I}_i,$$

$$\mathbf{K}_{II}^i = \begin{pmatrix} \mathbf{Q}_{II}^i & \mathbf{0} & (\mathbf{A}_{II}^i)^T \\ \mathbf{0} & \alpha \mathbf{R}_{II}^i & (\mathbf{B}_{II}^i)^T \\ \mathbf{A}_{II}^i & \mathbf{B}_{II}^i & \end{pmatrix}, \quad \mathbf{K}_{\Gamma I}^i = \begin{pmatrix} \mathbf{Q}_{\Gamma I}^i & \mathbf{0} & (\mathbf{A}_{I\Gamma}^i)^T \\ \mathbf{A}_{\Gamma I}^i & \mathbf{B}_{\Gamma I}^i & \end{pmatrix}.$$

Furthermore,

$$\mathbf{x}_\Gamma = \begin{pmatrix} \mathbf{y}_\Gamma \\ \mathbf{p}_\Gamma \end{pmatrix}, \mathbf{g}_\Gamma = \begin{pmatrix} \mathbf{c}_\Gamma \\ \mathbf{b}_\Gamma \end{pmatrix}, \quad \mathbf{x}_I^i = \begin{pmatrix} \mathbf{y}_I^i \\ \mathbf{u}_I^i \\ \mathbf{p}_I^i \end{pmatrix}, \mathbf{g}_I^i = \begin{pmatrix} \mathbf{c}_I^i \\ \mathbf{d}_I^i \\ \mathbf{b}_I^i \end{pmatrix}.$$

Frequently, we use the compact notation

$$\begin{pmatrix} \mathbf{K}_{II} & \mathbf{K}_{\Gamma I}^T \\ \mathbf{K}_{\Gamma I} & \mathbf{K}_{\Gamma\Gamma} \end{pmatrix} \begin{pmatrix} \mathbf{x}_I \\ \mathbf{x}_\Gamma \end{pmatrix} = \begin{pmatrix} \mathbf{g}_I \\ \mathbf{g}_\Gamma \end{pmatrix}, \tag{4.6}$$

or even $\mathbf{K}\mathbf{x} = \mathbf{g}$ instead of (4.5).

Assuming that $\mathbf{K}_{II}$ is invertible (we will present conditions that guarantee the invertibility in Theorem 4.2 below), we can form the Schur complement system

$$\mathbf{S}\mathbf{x}_\Gamma = \mathbf{r} \tag{4.7}$$

corresponding to (4.5), where

$$\mathbf{S} = \mathbf{K}_{\Gamma\Gamma} - \mathbf{K}_{\Gamma I}\mathbf{K}_{II}^{-1}\mathbf{K}_{\Gamma I}^T \tag{4.8}$$

and

$$\mathbf{r} = \mathbf{g}_\Gamma - \mathbf{K}_{\Gamma I}\mathbf{K}_{II}^{-1}\mathbf{g}_I.$$

Due to the block structure of $\mathbf{K}_{\Gamma I}$ and $\mathbf{K}_{II}$, the Schur complement $\mathbf{S}$ can be written as a sum of subdomain Schur complements,

$$\mathbf{S} = \sum_{i=1}^{s} \mathbb{I}_i^T \mathbf{S}_i \mathbb{I}_i, \tag{4.9}$$

where

$$\mathbf{S}_i = \mathbf{K}_{\Gamma\Gamma}^i - \mathbf{K}_{\Gamma I}^i (\mathbf{K}_{II}^i)^{-1} (\mathbf{K}_{\Gamma I}^i)^T, \quad i = 1, \ldots, s. \tag{4.10}$$

Similarly,

$$\mathbf{r} = \sum_{i=1}^{s} \mathbb{I}_i^T \mathbf{r}_i,$$

where $\mathbf{r}_i = \mathbf{g}_\Gamma^i - \mathbf{K}_{\Gamma I}^i (\mathbf{K}_{II}^i)^{-1} \mathbf{g}_I^i$, $i = 1, \ldots, s$.

Observe that

$$\mathbf{S}_i = \mathbf{H}_i^T \mathbf{K}^i \mathbf{H}_i, \tag{4.11}$$

where

$$\mathbf{H}_i = \begin{pmatrix} -(\mathbf{K}_{II}^i)^{-1}\mathbf{K}_{I\Gamma}^i \\ \mathbf{I} \end{pmatrix} \tag{4.12}$$

and

$$\mathbf{K}^i = \begin{pmatrix} \mathbf{K}_{II}^i & (\mathbf{K}_{\Gamma I}^i)^T \\ \mathbf{K}_{\Gamma I}^i & \mathbf{K}_{\Gamma\Gamma}^i \end{pmatrix}.$$

As before (see note below equation (4.10)), the application of $\mathbb{I}_i$ and $\mathbb{I}_i^T$ eliminate zero rows and columns.

The matrix $\mathbf{H}_i$ defined in (4.12) is the matrix representation of the operator $\mathcal{H}_i^h$ defined in (3.20). The representation (4.11) corresponds to the representation (3.21b) of the subdomain Schur complement operator $\mathcal{S}_i^h$.

The matrix $\mathbf{K}^i$ plays an important role for the computation of the inverse of $\mathbf{S}_i$ (assuming it exists), which will be used in Section 4.2 to precondition $\mathbf{S}$. In fact, if $\mathbf{K}_{II}^i$ is invertible,

$$\mathbf{K}^i = \begin{pmatrix} \mathbf{I} & \mathbf{0} \\ \mathbb{I}_i \mathbf{K}_{\Gamma I}^i (\mathbf{K}_{II}^i)^{-1} & \mathbf{I} \end{pmatrix} \begin{pmatrix} \mathbf{K}_{II}^i & \mathbf{0} \\ \mathbf{0} & \mathbf{S}_i \end{pmatrix} \begin{pmatrix} \mathbf{I} & (\mathbf{K}_{II}^i)^{-1} (\mathbf{K}_{\Gamma I}^i)^T \mathbb{I}_i^T \\ \mathbf{0} & \mathbf{I} \end{pmatrix} \tag{4.13}$$

and $\mathbf{S}_i$ is invertible if and only if $\mathbf{K}^i$ is invertible. In this case,

$$\mathbf{S}_i^{-1} \mathbf{v} = \begin{pmatrix} \mathbf{0} & \mathbf{I} \end{pmatrix} (\mathbf{K}^i)^{-1} \begin{pmatrix} \mathbf{0} \\ \mathbf{I} \end{pmatrix} \mathbf{v} \tag{4.14}$$

(see, e.g., [38, p. 113]). The previous formula is the algebraic version of Theorem 3.4.

We conclude this subsection with a result concerning the invertibility of the submatrices $\mathbf{K}_{II}^i$, which is important for the computation of $\mathbf{S}_i$, and with the invertibility of the submatrices $\mathbf{K}^i$, which is important for the computation of $(\mathbf{S}_i)^{-1}$. We set

$$\mathbf{A}^i = \begin{pmatrix} \mathbf{A}_{II}^i & \mathbf{A}_{I\Gamma}^i \\ \mathbf{A}_{\Gamma I}^i & \mathbf{A}_{\Gamma\Gamma}^i \end{pmatrix}.$$

Matrices $\mathbf{Q}^i, \mathbf{R}^i$ are defined analogously.

Before we state our result on the invertibility of $\mathbf{K}_{II}^i$ and $\mathbf{K}^i$, we recall the following theorem, which is proven, e.g., in [14].

Theorem 4.1 *Let $\mathbf{A} \in \mathbb{R}^{m\times m}, \mathbf{B} \in \mathbb{R}^{m\times n}$ be arbitrary matrices and let $\mathbf{Q} \in \mathbb{R}^{m\times m}, \mathbf{R} \in \mathbb{R}^{n\times n}$ be symmetric. If*

$$\mathit{range}(\mathbf{A} \mid \mathbf{B}) = \mathbb{R}^m \tag{4.15}$$

and if

$$\begin{pmatrix} \mathbf{z} \\ \mathbf{v} \end{pmatrix}^T \begin{pmatrix} \mathbf{Q} & \mathbf{0} \\ \mathbf{0} & \alpha\mathbf{R} \end{pmatrix} \begin{pmatrix} \mathbf{z} \\ \mathbf{v} \end{pmatrix} > 0 \tag{4.16}$$

for all $\mathbf{z} \in \mathbb{R}^m, \mathbf{v} \in \mathbb{R}^n$ with $\mathbf{Az} + \mathbf{Bv} = 0$ and $(\mathbf{z}^T, \mathbf{v}^T) \neq 0$, then

$$\begin{pmatrix} \mathbf{Q} & \mathbf{0} & \mathbf{A}^T \\ \mathbf{0} & \alpha\mathbf{R} & \mathbf{B}^T \\ \mathbf{A} & \mathbf{B} & \mathbf{0} \end{pmatrix}$$

has $m+n$ positive eigenvalues and m negative eigenvalues.

Theorem 4.2 *i. The matrices* $\mathbf{Q}^i_{II}, \mathbf{R}^i_{II}$ *are symmetric positive definite. If* (2.3a), (2.3b), (2.3d) *hold, and if the stabilization parameter* τ_e *is sufficiently small, the matrix* $\mathbf{A}^i_{II}$ *obeys* $\mathbf{v}^T\mathbf{A}^i_{II}\mathbf{v} > 0$ *for all* $\mathbf{v} \neq 0$ *and* $\mathbf{K}^i_{II}$ *is invertible.*

ii. The matrices $\mathbf{Q}^i, \mathbf{R}^i$ *are symmetric positive definite. If* (2.3a)–(2.3c) *hold and if the stabilization parameter* τ_e *is sufficiently small, the matrix* $\mathbf{A}^i$ *obeys* $\mathbf{v}^T\mathbf{A}^i\mathbf{v} > 0$ *for all* $\mathbf{v} \neq 0$ *and* $\mathbf{K}^i$ *is invertible.*

iii. If (2.3a), (2.3b), (2.3d) *hold, if the relative interior of* $\partial\Omega_i \cap \partial\Omega_D$ *is nonempty, and if the stabilization parameter* τ_e *is sufficiently small, the matrix* $\mathbf{A}^i$ *obeys* $\mathbf{v}^T\mathbf{A}^i\mathbf{v} > 0$ *for all* $\mathbf{v} \neq 0$ *and* $\mathbf{K}^i$ *is invertible.*

Proof: i. Using the definitions (3.9) and (3.10) and the assumptions (2.3a), (2.3b), (2.3d) we have

$$\begin{aligned} a_{i,h}(v_h, v_h) &= \int_{\Omega_i} \varepsilon\nabla v_h(x)\cdot\nabla v_h(x) + (r(x) - \tfrac{1}{2}\nabla\cdot\mathbf{a}(x))v_h^2(x)dx \\ &\quad + \tfrac{1}{2}\int_{\partial\Omega_i\cap\partial\Omega_N} \mathbf{a}(x)\cdot\mathbf{n}_i v_h^2(x)dx, \\ &\quad + \sum_{T_e\in\overline{\Omega_i}} \tau_e\langle -\varepsilon\Delta v_h + \mathbf{a}\cdot\nabla v_h + r v_h, \mathbf{a}\cdot\nabla v_h\rangle_{T_e} \\ &\geq \varepsilon|\nabla v_h|_{1,\Omega_i} + r_0\|v_h\|_{0,\Omega_i} \\ &\quad + \sum_{T_e\in\overline{\Omega_i}} \tau_e\langle -\varepsilon\Delta v_h + \mathbf{a}\cdot\nabla v_h + r v_h, \mathbf{a}\cdot\nabla v_h\rangle_{T_e} \end{aligned}$$

for all $v_h \in Y^h_{i,0}$. (Note that for $v_h \in Y^h_{i,0}$ we have $a_{i,h}(v_h, v_h) = \widetilde{a}_{i,h}(v_h, v_h)$, i.e., the modification of the local bilinear from (3.9) is not important here.) Standard SUPG estimates (cf. [25, p. 378] or [34, L. 3.28,p. 231]) show that

$$a_{i,h}(v_h, v_h) \geq \frac{\varepsilon}{2}|\nabla v_h|_{1,\Omega_i} + \frac{r_0}{2}\|v_h\|_{0,\Omega_i} + \frac{1}{2}\sum_{T_e\in\overline{\Omega_i}} \tau_e\|\mathbf{a}\cdot\nabla v_h\|_{0,T_e}$$

for all $v_h \in Y^h_{i,0}$. By a Poincaré inequality, we have $\|v_h\|_{0,\Omega_i} \leq c|\nabla v_h|_{1,\Omega_i}$. Hence,

$$\mathbf{v}^T\mathbf{A}^i_{II}\mathbf{v} = a_{i,h}(v_h, v_h) \geq \frac{\varepsilon}{2}|\nabla v_h|_{1,\Omega_i} + \frac{r_0}{2}\|v_h\|_{0,\Omega_i} + \frac{1}{2}\sum_{T_e\in\overline{\Omega_i}} \tau_e\|\mathbf{a}\cdot\nabla v_h\|_{0,T_e} > 0$$

for all $\mathbf{v} \neq 0$. In particular $\mathbf{A}^i_{II}$ is invertible and (4.15) with $\mathbf{A}$, $\mathbf{B}$, m replaced by $\mathbf{A}^i_{II}$, $\mathbf{B}^i_{II}$, m^i_I, respectively, is valid. Moreover, the matrices $\mathbf{Q}^i_{II} \in \mathbb{R}^{m^i_I\times m^i_I}$ $\mathbf{R}^i_{II} \in \mathbb{R}^{n^i\times n^i}$ are subdomain mass matrices, which implies their symmetric positive definiteness. Hence (4.16) with $\mathbf{Q}, \mathbf{R}$ replaced by $\mathbf{Q}^i_{II}, \mathbf{R}^i_{II}$ is valid for all $\mathbf{z} \in \mathbb{R}^{m^i_I}, \mathbf{v} \in \mathbb{R}^{n^i}$ with $(\mathbf{z}^T, \mathbf{v}^T) \neq 0$. The result now follows from Theorem 4.1.

ii. We proceed as in the first part to show that

$$a_{i,h}(v_h, v_h) \geq \frac{\varepsilon}{2}|\nabla v_h|_{1,\Omega_i} + \frac{r_0}{2}\|v_h\|_{0,\Omega_i} + \frac{1}{2}\sum_{T_e \in \overline{\Omega_i}} \tau_e \|\mathbf{a}\cdot\nabla v_h\|_{0,T_e} \quad \forall v_h \in Y_i^h.$$

Hence, $\mathbf{v}^T\mathbf{A}^i\mathbf{v} > 0$ for all $\mathbf{v} \neq 0$. We can now proceed as in part i. to prove the invertibility of $\mathbf{K}^i$.

iii. If the relative interior of $\partial\Omega_i \cap \partial\Omega_D$ is nonempty, then due to a Poincaré inequality there exists a constant $c > 0$ such that $\|v_h\|_{0,\Omega_i} \leq c|\nabla v_h|_{1,\Omega_i}$ for all $v_h \in Y_i^h$ and we can admit $r_0 = 0$ in part ii. □

Remark 4.3 *i. Examination of the proof of Theorem* 4.2 *reveals the importance of the modification* (3.9) *of the local bilinear form to guarantee* $a_{i,h}(v_h, v_h) > 0$ *for all* $v_h \in Y_i^h, v_h \neq 0$, *i.e.,* $\mathbf{v}^T\mathbf{A}^i\mathbf{v} > 0$ *for all* $\mathbf{v} \neq 0$.

ii. Just to guarantee the invertibility of $\mathbf{K}^i$, *the conditions in Theorem* 4.2*ii, iii. may be too strong.*

For our model problem with distributed control, $\mathbf{B}^i \in \mathbb{R}^{m^i \times n^i}$, *with* $n^i > m^i$, *is related to the mass matrix and satisfies* $rank(\mathbf{B}^i) = \mathbb{R}^{m^i}$. *Hence,* (4.15) *is satisfied. (The invertibility of* $\mathbf{A}^i$ *is not needed.) Moreover,* $\mathbf{Q}^i, \mathbf{R}^i$ *are subdomain mass matrices, and, hence,*

$$\begin{pmatrix} \mathbf{z} \\ \mathbf{v} \end{pmatrix}^T \begin{pmatrix} \mathbf{Q}^i & \mathbf{0} \\ \mathbf{0} & \alpha\mathbf{R}^i \end{pmatrix} \begin{pmatrix} \mathbf{z} \\ \mathbf{v} \end{pmatrix} > 0 \quad \textit{for all } \mathbf{z} \in \mathbb{R}^{m^i}, \mathbf{v} \in \mathbb{R}^{n^i} \textit{ with } (\mathbf{z}^T, \mathbf{v}^T) \neq 0.$$

This means that for our model problem with distributed control, the invertibility of $\mathbf{A}^i$ *is not needed to ensure the invertibility of* $\mathbf{K}^i$*! In particular,* $\mathbf{K}^i$ *is also invertible if we use the local bilinear form* (3.8) *instead of* (3.9).

4.2 The Robin-Robin Preconditioners

It is now relatively easy to generalize the Robin-Robin preconditioner used in the context of advection dominated elliptic PDEs [4] to the optimal control context.

Let $\mathbf{D}_i^y$ be the diagonal matrix, whose entries are computed as follows. If the node x_k satisfies $x_k \in \Gamma_i$, then $(\mathbf{D}_i^y)_{kk}^{-1}$ is the number of subdomains that share node x_k. Note that $\sum_i \mathbf{D}_i^y = \mathbf{I}$. Furthermore, let $\mathbf{D}_i^p = \tilde{\mathbf{D}}_i^y$ and

$$\mathbf{D}_i = \begin{pmatrix} \mathbf{D}_i^y & \\ & \mathbf{D}_i^p \end{pmatrix}.$$

By Theorem 4.2 i. $\mathbf{S}_i$, $i = 1,\ldots,s$, is well defined. The one-level Robin-Robin preconditioner is given by

$$\mathbf{P} = \sum_i \mathbf{D}_i \mathbb{I}_i^T \mathbf{S}_i^{-1} \mathbb{I}_i \mathbf{D}_i. \tag{4.17}$$

In principle it is possible to incorporate a coarse space, but this has not yet been been explored in the optimal control context.

4.3 Implementation

Instead of working on the preconditioned Schur complement system

$$\mathbf{PSx}_\Gamma = \mathbf{P}(\mathbf{g}_\Gamma - \mathbf{K}_{\Gamma I}\mathbf{K}_{II}^{-1}\mathbf{g}_I) = \mathbf{Pr}. \tag{4.18}$$

we work on the preconditioned full system. It is easy to verify that

$$\begin{pmatrix} \mathbf{K}_{II} & \mathbf{K}_{\Gamma I}^T \\ \mathbf{K}_{\Gamma I} & \mathbf{K}_{\Gamma\Gamma} \end{pmatrix} = \underbrace{\begin{pmatrix} \mathbf{K}_{II} & 0 \\ \mathbf{K}_{\Gamma I} & \mathbf{P}^{-1} \end{pmatrix}}_{=(\mathbf{P}_l^K)^{-1}} \begin{pmatrix} \mathbf{I} & 0 \\ 0 & \mathbf{PS} \end{pmatrix} \underbrace{\begin{pmatrix} \mathbf{I} & \mathbf{K}_{II}^{-1}\mathbf{K}_{\Gamma I}^T \\ 0 & \mathbf{I} \end{pmatrix}}_{=(\mathbf{P}_r^K)^{-1}}. \tag{4.19}$$

We will look at the preconditioned system

$$\mathbf{P}_l^K \mathbf{K} \mathbf{P}_r^K \widehat{\mathbf{x}} = \mathbf{P}_l^K \mathbf{g}, \tag{4.20}$$

where $\widehat{\mathbf{x}} = (\mathbf{P}_r^K)^{-1}\mathbf{x}$, and at the preconditioned Schur complement system (4.18). Consider an initial iterate

$$\mathbf{x}^0 = \begin{pmatrix} \mathbf{x}_I^0 \\ \mathbf{x}_\Gamma^0 \end{pmatrix}, \tag{4.21}$$

with

$$\mathbf{x}_I^0 = \mathbf{K}_{II}^{-1}(\mathbf{g}_I - \mathbf{K}_{\Gamma I}^T \mathbf{x}_\Gamma^0) \tag{4.22}$$

and set $\widehat{\mathbf{x}}^0 = (\mathbf{P}_r^K)^{-1}\mathbf{x}^0$. The corresponding preconditioned residual satisfies

$$\widehat{\mathbf{r}}^0 = \mathbf{P}_l^K(\mathbf{g} - \mathbf{K}\mathbf{P}_r^K)\widehat{\mathbf{x}}^0 = \begin{pmatrix} 0 \\ \mathbf{P}(\mathbf{g}_\Gamma - \mathbf{K}_{\Gamma I}\mathbf{K}_{II}^{-1}\mathbf{g}_I - \mathbf{S}\mathbf{x}_\Gamma^0) \end{pmatrix} = \begin{pmatrix} 0 \\ \widehat{\mathbf{r}}_\Gamma^0 \end{pmatrix}. \tag{4.23}$$

We see that the second component of the initial residual $\widehat{\mathbf{r}}^0$ of the preconditioned system (4.20) is the initial residual $\widehat{\mathbf{r}}_\Gamma^0 = \mathbf{P}(\mathbf{g}_\Gamma - \mathbf{K}_{\Gamma I}\mathbf{K}_{II}^{-1}\mathbf{g}_I - \mathbf{S}\mathbf{x}_\Gamma^0)$ of the preconditioned Schur complement system (4.18).

Recall that for a matrix A and a vector v, the Krylov subspace is defined by $\mathcal{K}_k(A,v) = \text{span}\{v, Av, \ldots, A^{k-1}v\}$. Using the fact that the first component of $\widehat{\mathbf{r}}^0$ is zero and that $\mathbf{P}_l^K\mathbf{K}\mathbf{P}_r^K$ is a block diagonal matrix, we immediately obtain the following relation between the Krylov subspaces of the preconditioned system (4.20) and the preconditioned Schur complement system (4.18):

$$\mathcal{K}_k(\mathbf{P}_l^K\mathbf{K}\mathbf{P}_r^K, \widehat{\mathbf{r}}^0) = \{0\} \times \mathcal{K}_k(\mathbf{PS}, \widehat{\mathbf{r}}_\Gamma^0) \quad \forall k. \tag{4.24}$$

This relationship allows one to establish relationships between Krylov subspace methods applied to the preconditioned Schur compement system (4.18) and the preconditioned full system (4.20), provided that the initial iterates satisfy (4.22). For the symmetric positive definite case see [24]. If the application of $\mathbf{K}_{II}^{-1}$ is exact, there is no difference between the solution of preconditioned Schur complement system (4.18) and the preconditioned full system (4.20). However, the latter provides advantages if the application of $\mathbf{K}_{II}^{-1}$ is performed inexactly using iterative methods [24, 18]. In our numerical examples, we solve systems of the form $\mathbf{K}_{II}^{i}\mathbf{v}_{I}^{i} = \mathbf{r}_{I}^{i}$ and $\mathbf{K}^{i}\mathbf{v}^{i} = \mathbf{r}^{i}$ (the latter arising in the application of our preconditioner, cf. (4.14)) exactly (up to floating point arithmetic) using UMFPACK 4.3 [9]. Still, we work with the the preconditioned full system (4.20) to allow the incorporation of iterative solvers in the future.

In our numerical experiments reported on in the next section, we use GMRES [35] and sQMR [11, 12] applied to

$$\mathbf{P}_r^K \mathbf{P}_l^K \mathbf{K}\mathbf{x} = \mathbf{P}_r^K \mathbf{P}_l^K \mathbf{g}. \tag{4.25}$$

We have observed that the number of GMRES [sQMR] iterations applied to (4.20) is close to the number of GMRES [sQMR] iterations applied to (4.25). In both cases GMRES [sQMR] was stopped if the respective preconditioned residual was reduced by a factor of 10^{-9}. However, we also observed that the error between the solution computed using GMRES and the exact solution $\mathbf{K}^{-1}\mathbf{g}$ was for small diffusion ε significantly smaller when left preconditioning (4.25) was used instead of split preconditioning (4.20). This is not surprising, since the GMRES iteration is stopped when the preconditioned residual $\|\mathbf{P}_r^K \mathbf{P}_l^K \mathbf{K}\mathbf{x} - \mathbf{P}_r^K \mathbf{P}_l^K \mathbf{g}\|$ or $\|\mathbf{P}_l^K \mathbf{K}\mathbf{x} - \mathbf{P}_l^K \mathbf{g}\|$, respectively, is small and the matrix $\mathbf{P}_r^K \mathbf{P}_l^K \mathbf{K}$ is expected to have a smaller condition number than $\mathbf{P}_l^K \mathbf{K}$. The error between the solution computed using sQMR applied to (4.25) and the exact solution $\mathbf{K}^{-1}\mathbf{g}$ was observed to be also smaller than the error between the solution computed using sQMR applied to (4.20) and the exact solution $\mathbf{K}^{-1}\mathbf{g}$, but the differences were much smaller than those observed for GMRES.

5 Numerical Results

In this section we illustrate the performance of our optimization-level domain decomposition method for several advection dominated optimal control problems with distributed controls or with boundary controls.

To explore the importance of the modification (3.9) of the local bilinear form, we run experiments with and without this modification. If we use the modified local bilinear form (3.9), then we refer to the resulting preconditioner as a Robin–Robin (R–R) preconditioner. This name is motivated by the Robin transmission conditions (3.16) for the state (and the adjoint) and the Robin boundary conditions for the state (and the adjoint) in the subproblem (3.30) for the inversion of $\mathcal{S}_i$. If $a_i(y_h, \phi_h) = \widetilde{a}_i(y_h, \phi_h)$, i.e., no modification of the local bilinear form is applied, then we refer to the resulting preconditioner as a Neumann–Neumann (N–N) preconditioner. This name is motivated by the Neumann transmission

conditions (3.19) for the state and the Neumann boundary conditions for the state in the subproblem (3.32) for the inversion of $\mathcal{S}_i$.

5.1 Distributed Control

5.1.1 Influence of Different Velocity Fields

This example is derived from Example 4.1 in [4]. We use $\Omega = (0,1) \times (0,0.2)$, $\partial\Omega_D = \partial\Omega$, $r = 1$, $f = 0$, and one of the following four advections $\mathbf{a}(x) = \mathbf{e}_1$, $\mathbf{a}(x) = \mathbf{e}_2$, $\mathbf{a}(x) = (1/\sqrt{2})(\mathbf{e}_1 + \mathbf{e}_2)$, or $\mathbf{a}(x) = 2\pi((x_1 - 0.5)\mathbf{e}_2 + (x_2 - 0.1)\mathbf{e}_1)$. These are refered to as 'normal', 'parallel', 'oblique', and 'rotating', respectively. We generate $\hat{y}$ as the solution of

$$-\varepsilon\Delta\hat{y}(x) + \mathbf{a}(x)\cdot\nabla\hat{y}(x) + \hat{y}(x) = 5e^{-\frac{(x_1-0.2)^2+(x_2-0.1)^2}{2\cdot 0.1^2}} + 5e^{-\frac{(x_1-0.8)^2+(x_2-0.1)^2}{2\cdot 0.1^2}}, \quad x \in \Omega, \tag{5.1a}$$

$$\hat{y}(x) = 0, \quad x \in \partial\Omega. \tag{5.1b}$$

We decompose Ω into 5 subdomains of size $(0,0.2) \times (0,0.2)$. Each subdomain is triangulated by dividing each axis into 30 subintervals and subsequently subdividing the resulting rectangles into two triangles. The problems are solved by a preconditioned sQMR algorithm where the stopping criterion is to reduce the initial residual by a factor of 10^{-9}. We use either Robin–Robin (R–R) or Neumann–Neumann (N–N) preconditioning.

Unlike in the PDE-only case in [4], the unpreconditioned sQMR (the same is true for GMRES) fails to reduce the initial residual to the specified tolerance within 1000 iterations for all experiments outlined below. Therefore, we do not give any further numerical results in absence of preconditioning. In Tables 5.1 and 5.2 we report the number of preconditioned sQMR iterations for the values $\alpha = 10^{-4}$ and $\alpha = 1$ of the regularization parameter, respectively.

We recall (cf. Remark 4.3) that for the distribruted control case the invertibility of $\mathbf{A}^i$, i.e., the modification (3.9) of the bilinear form is not needed to ensure invertibility of $\mathbf{K}^i$ and, hence $\mathbf{S}_i$. Thus the application of the Neumann–Neumann (N–N) preconditioner is well–posed for the distributed control case.

Tables 5.1 and 5.2 show that for large ε, both Robin–Robin and Neumann–Neumann preconditioners perform equally well, with all sQMR runs finishing in 4 iterations. This is in agreement with the PDE-only case reported in [4, Table 1]. When the velocity is parallel to subdomain interfaces, then $a_i(y_h, \phi_h) = \widetilde{a}_i(y_h, \phi_h)$ and the Robin–Robin and the Neumann-Neumann are identical. The Robin–Robin preconditioner adapts nicely to small ε for all velocities. The performance of the Neumann–Neumann preconditioner deteriorates with decreasing ε, but this deterioration is not nearly as pronounced as in the PDE-only case in [4, Table 1]. Finally, we observe that the size of the regularization parameter α seems to

ε	Prec. \ Velocity	Normal	Parallel	Oblique	Rotating
0.001	R-R	12	3	13	9
	N-N	21	3	18	13
1	R-R	4	4	4	4
	N-N	4	4	4	4

Table 5.1. sQMR iterations for different velocity fields and fixed regularization parameter $\alpha = 10^{-4}$.

ε	Prec. \ Velocity	Normal	Parallel	Oblique	Rotating
0.001	R-R	12	3	4	6
	N-N	53	3	30	14
1	R-R	4	4	4	4
	N-N	4	4	4	4

Table 5.2. sQMR iterations for different velocity fields and fixed regularization parameter $\alpha = 1$.

affect the performance of both preconditioners only moderately. This observation is further examined in Example 5.1.2.

5.1.2 Influence of the Number of Subdomains, Grid Sizes, and Regularization

The purpose of this example is to assess the sensitivity of the Robin–Robin and Neumann–Neumann preconditioners to increases in the number of subdomains and grid points.

We use $\Omega = (0,1) \times (0,1)$, $\partial\Omega_D = \partial\Omega$, $\varepsilon = 0.001$, $\mathbf{a}(x) = 3\mathbf{e}_1$ $r = 1$, and $f = 0$. We generate $\hat{y}$ as in Example 5.1.1 but with a minor modification in the second term in the right hand side. Specifically, $\hat{y}$ is computed as the solution of

$$-\varepsilon\Delta\hat{y}(x) + \mathbf{a}(x)\cdot\nabla\hat{y}(x) + \hat{y}(x) = 5e^{-\frac{(x_1-0.2)^2+(x_2-0.1)^2}{2\cdot 0.1^2}} + 5e^{-\frac{(x_1-0.8)^2+(x_2-0.9)^2}{2\cdot 0.1^2}}, \qquad x \in \Omega, \tag{5.2a}$$

$$\hat{y}(x) = 0, \qquad x \in \partial\Omega. \tag{5.2b}$$

For the first experiment we use a fixed uniform grid of size 128×128 (note that each square in the mesh is divided into two triangles). The grid is partitioned in various ways. First, we use 4, 8, and 16 vertical rectangular strips of equal size (yielding subdomain

sizes of 32×128, 16×128, and 8×128, respectively). Second, we partition the grid into 2×2, 4×4, 8×8, and 16×16 square subdomains (with sudomain sizes of 64×64, 32×32, 16×16, and 8×8 respectively). Finally, the grid is subdivided into 16 horizontal rectangular strips of equal size (yielding a subdomain size of 128×8). The results are presented in Table 5.3.

Reg.	Prec. \ Part.	4×1	8×1	16×1	1×16
$\alpha = 10^{-4}$	R-R	12	12	14	3
	N-N	39	39	38	3
$\alpha = 1$	R-R	9	19	38	3
	N-N	130	361	> 500	3

Reg.	Prec. \ Part.	2×2	4×4	8×8	16×16
$\alpha = 10^{-4}$	R-R	13	15	17	21
	N-N	35	44	46	49
$\alpha = 1$	R-R	7	14	24	47
	N-N	87	172	452	> 500

Table 5.3. sQMR iterations for varying numbers of subdomains and fixed diffusivity $\varepsilon = 0.001$.

Table 5.3 shows that for large α, the number of sQMR iterations roughly doubles as the number of subdomains in x_1-direction doubles, for both preconditioners. This is also observed in [4, Table 2]. The Robin–Robin preconditioner performs better than the Neumann-Neumann preconditioner. For large α the performance differences are as pronounced as in the PDE-only case reported in [4].

For small α, the number of sQMR iterations does not increase significantly as the number of subdomains is increased (regardless of the position of subdomain interfaces). This is a surprising and not yet understood result, which unfortunately does not hold true for most other problem setups with complex velocity fields (see the following examples). The Neumann–Neumann preconditioner performs much better here than in the case of large α.

For partitions in which all subdomain interfaces are parallel to the velocity field, i.e., 1×4, 1×8, and 1×16 partitions, the number of sQMR iterations is not affected at all by the number of subdomains or the size of the regularization parameter. Both Robin–Robin and Neumann–Neumann preconditioned sQMR runs complete all tests in only 3 iterations (the 1×4 and 1×8 results are not tabulated).

The second experiment examines the influence of the number of grid points. The problem is set up as in the first experiment, except that here we fix two particular subdomain partitions, and vary the grid size. We use either an 8×1 rectangular subdomain partition or a 4×4 square subdomain partition, on uniform grids of sizes 32×32, 64×64, and

128×128 (again, each mesh square is split into two triangular elements). The results are presented in Table 5.4.

		8×1 Partition		
Reg.	Prec. \ Grid Size	32×32	64×64	128×128
$\alpha = 10^{-4}$	R-R	15	12	12
	N-N	21	27	39
$\alpha = 1$	R-R	21	19	19
	N-N	307	368	361

		4×4 Partition		
Reg.	Prec. \ Grid Size	32×32	64×64	128×128
$\alpha = 10^{-4}$	R-R	16	16	15
	N-N	28	33	44
$\alpha = 1$	R-R	16	15	14
	N-N	143	156	172

Table 5.4. sQMR iterations for varying numbers of grid points and fixed diffusivity $\varepsilon = 0.001$.

They indicate that the convergence of the sQMR algorithm with the Robin–Robin preconditioner is not affected by the grid size. This agrees with the results stated in [4, Table 5]. On the other hand, the performance of the Neumann-Neumann preconditioned algorithm deteriorates slightly as the number of grid points is increased. The size of the regularization parameter α does not affect the performance of the Robin–Robin preconditioner. In contrast, for large α the Neumann-Neumann preconditioner performs extremely poorly for all grid sizes.

5.2 Source Inversion

This example is motivated by the desire to identify the source of a hazardous material from measurements of the concentration at sensor locations $x_1^s, \ldots, x_{N_s}^s$. The problem is modeled as

$$\text{minimize } \frac{1}{2}\sum_{j=1}^{N_s}(y(x_j^s)-\widehat{y}_j)^2 dx + \frac{\alpha}{2}R(u) \tag{5.3a}$$

subject to

$$-\varepsilon\Delta y(x) + \mathbf{a}(x)\cdot\nabla y(x) = u(x), \qquad x\in\Omega, \tag{5.3b}$$

$$y(x) = 0, \qquad x\in\partial\Omega_D, \tag{5.3c}$$

$$\varepsilon\frac{\partial}{\partial\mathbf{n}}y(x) = 0, \qquad x\in\partial\Omega_N. \tag{5.3d}$$

Here $x_1^s, \ldots, x_{N_s}^s$ are the sensor locations, u represents the unknown source, y represents the concentration, and $\widehat{y}_j$ are the concentration measurements at the sensor locations. In (5.3a), the term $R(u)$ represents a regularization term. We use

$$R(u) = \int_\Omega u^2(x)\,dx, \quad \text{or} \quad R(u) = \int_\Omega \nabla u(x)\cdot\nabla u(x)\,dx.$$

It is not our intention to examine this example from an inverse problem point of view ([5, 40]), i.e., study the quality of the source estimate u obtained from (5.3), the choice of the regularization term R or the regularization parameter α. We focus on the solution of (5.3) for given $\alpha > 0$ and R. Since we use pointwise observations in (5.3a) and may only include a seminorm regularization, $\int_\Omega \nabla u(x)\cdot\nabla u(x)\,dx$, the existence and uniqueness result in Theorem 2.1 does not apply here and we proceed formally.

The problem domain Ω is sketched in Figure 5.1 and represents the cross section of a two-story building.

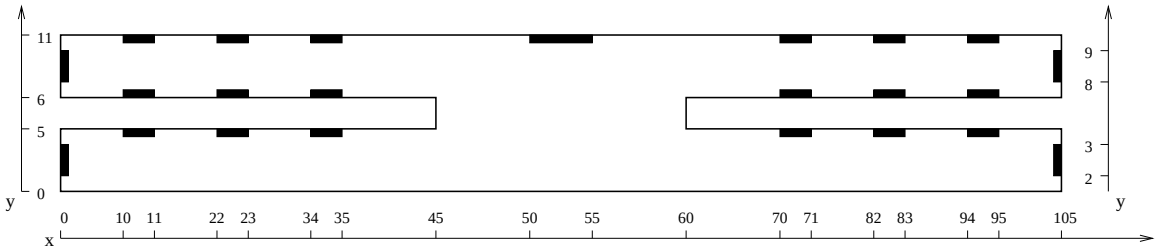

Figure 5.1. Problem geometry, vent placement. (All measurements are in meters, not to scale).

The advection **a** in (5.3a) is obtained is obtained from a rough model of the air flow generated by an HVAC (heating-venting-air-conditioning) system. Air is blown into or out

of the building through vents, with locations indicated in Figure 5.1. Vents at the ceiling of the second story of the building (vents with y-coordinate $y = 11$) are outflow vents; air is blown into the building through all other vents. We use the Stokes equation to model the air flow in the building. Since our focus is on the performance of the domain decomposition preconditioner on (5.3), this model is sufficient for our pusposes. For more realistic models for indoor flows see, e.g., [27, 26, 33] and the references therein.

Our advection $\mathbf{a}$ is computed as the solution $\mathbf{a} = \mathbf{v}$ of

$$
\begin{aligned}
-\rho\mu\Delta\mathbf{v} + \nabla p &= \mathbf{0}, && \text{in } \Omega && (5.4a)\\
\nabla\cdot\mathbf{v} &= 0, && \text{in } \Omega && (5.4b)\\
\mathbf{v} &= -v_{in}\mathbf{n}, && \text{on } \Gamma_{in} && (5.4c)\\
\mathbf{v} &= v_{out}\mathbf{n}, && \text{on } \Gamma_{out,1} && (5.4d)\\
\rho\mu\nabla\mathbf{v}\mathbf{n} + p\mathbf{n} &= 0, && \text{on } \Gamma_{out,2} && (5.4e)\\
\mathbf{v} &= 0, && \text{on } \partial\Omega \setminus \{\Gamma_{in}\cup\Gamma_{out,1}\cup\Gamma_{out,2}\}. && (5.4f)
\end{aligned}
$$

The six small vents in the ceiling of the second floor indicated in Figure 5.1 describe the outflow boundary $\Gamma_{out,1}$. The outflow boundary $\Gamma_{out,1}$ is given by the opening $(50,55)\times\{11\}$ in the ceiling of the second floor. The remaining sixteen vents form the inflow boundary Γ_{in}. As before, $\mathbf{n}$ denotes the unit outward normal. To generate the flow field $\mathbf{a} = \mathbf{v}$ we use the following data. The density coefficient is $\rho = 1.25$ [kg/m^3], and the viscosity is $\mu = 1.8\times10^{-5}$. The inflow air speed is $v_{in} = 0.1$ [m/sec] for all inlets, and the outflow air speed $v_{out} = 0.2$ [m/sec] for the six smaller outlet vents. We use Taylor Hood finite elements to solve (5.4). The computed flow field for a mesh with 4492 nodes and 8324 triangles is depicted in Figure 5.2.

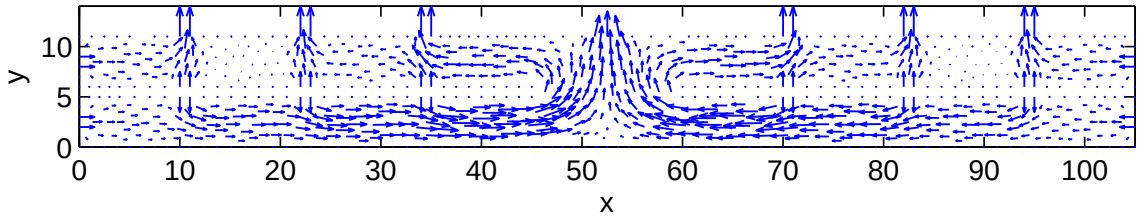

Figure 5.2. The HVAC flow.

For the source inversion problem (5.3), all inlets are subject to homogeneous Dirichlet boundary conditions, and all outlets and walls are assigned homogeneous Neumann boundary conditions. Thus the boundary segments in (5.3) and (5.4) are related as follows: $\partial\Omega_N = \partial\Omega\setminus\Gamma_{in}$, $\partial\Omega_D = \Gamma_{in}$. The sensors are distributed 'uniformly' throughout the mesh, and are placed at the node locations, which eliminates the need for interpolation of their positions relative to the mesh nodes. This sensor placement is done for computational convenience, but is not necessary. For illustrational purposes, a sample mesh with about 1000 nodes and 100 sensors is presented in Figure 5.3.

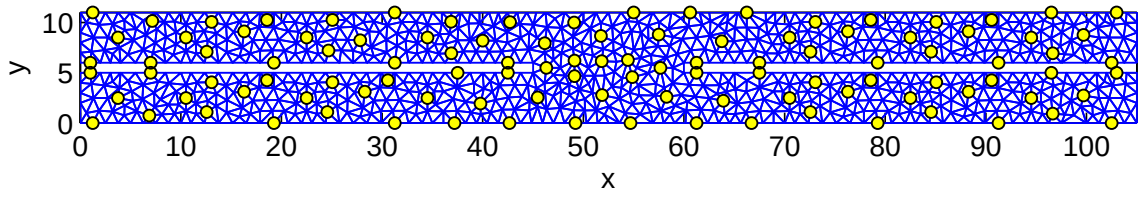

Figure 5.3. A sample finite-element mesh and sensor locations.

We generate sensor measurements by solving (5.3b–d) using a given right hand side

$$u(x) = 5\exp\left(-\frac{(x_1-25)^2+(x_2-2)^2}{2\cdot 0.7^2}\right) + 5\exp\left(-\frac{(x_1-90)^2+(x_2-8)^2}{2\cdot 0.7^2}\right)$$

i.e., two Gaussian sources of equal magnitude, one on each floor, in different locations.

Since $\mathbf{a} = \mathbf{v}$ solves (5.4) and $r = 0$, we have $r(x) - \frac{1}{2}\nabla\cdot\mathbf{a}(x) = 0$ a.e. in Ω. Moreover since homogeneous Neumann boundary conditions are assigned at all outlets and at walls, $\Omega_N = \partial\Omega \setminus \Gamma_{in}$, the boundary conditions (5.4d,f) imply that $\mathbf{a}\cdot\mathbf{n} \geq 0$ on $(\partial\Omega \setminus \{\Gamma_{in} \cup \Gamma_{out,1}\}$. On $\Gamma_{out,2}$ the computed velocity obeys $\mathbf{a}\cdot\mathbf{n} \geq 0$ (see also Figure 5.2).

We generate meshes using Triangle [37] and partition meshes using METIS [23]. For partitions into 16 or 32 subdomains, some subdomains do not contain inlet vents, i.e., do not contain boundary segments with Dirichlet boundary conditions. In these cases, Theorem 4.2ii,iii. cannot be applied to justify the invertibility of $\mathbf{K}^i$ corresponding to the subdomains that do not contain boundary segments with Dirichlet boundary conditions. Numerically, however, the solution of linear systems with $\mathbf{K}^i$, which is needed to apply $\mathbf{S}_i^{-1}$ (cf. (4.13)), did not pose problems. We conjecture that because of reasons similar to Remark 4.3 these $\mathbf{K}^i$'s are invertible.

For the first two experiments we choose a triangulation with 983 nodes, 1642 triangles, and 351 uniformly distributed sensors. The first experiment assesses the sensitivity of the Robin–Robin preconditioner with respect to decreasing diffusion coefficients. We use a regularization parameter of $\alpha = 10^{-5}$, 8 subdomains, and a relative residual stopping tolerance for sQMR of 10^{-9}. The results are depicted in Figure 5.4. We note that, as expected, the number of iterations increases only moderately as the problem becomes advection dominated (and thus much harder to solve). The second experiment assesses the robustness of the Robin–Robin preconditioner with respect to different regularization parameters. Here, the diffusion is set to $\varepsilon = 5\times 10^{-4}$, and the remaining problem parameters are as in the first experiment. From Figure 5.5 we observe that the regularization parameter has virtually no effect on the number of sQMR iterations. This agrees with a previous result for nonadvective quadratic elliptic problems [19].

The third experiment shows the influence of the number of subdomains and the number of grid points on Robin–Robin and Neumann-Neumann preconditioners. As in the first

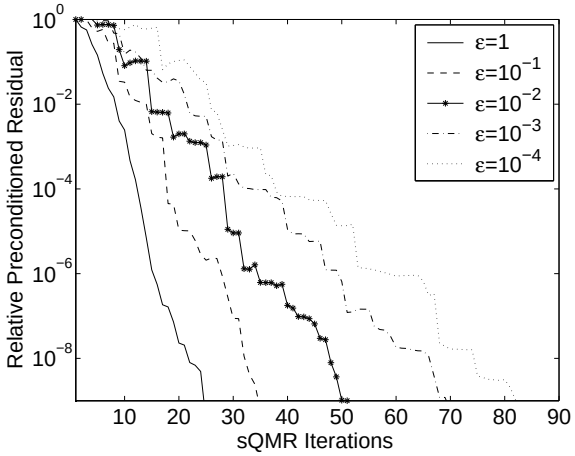

Figure 5.4. Influence of the diffusion ε on the R–R prec., for a fixed regularization $\alpha = 10^{-5}$.

two experiments, we use 351 uniformly distributed sensors. The diffusion is $\varepsilon = 5 \times 10^{-4}$, the regularization is $\alpha = 10^{-5}$, and the relative residual stopping tolerance is 10^{-9}. We observe from Table 5.5 that for the Robin–Robin preconditioner the number of sQMR iterations is only mildly affected by the number of grid points, with no clear dependence between them. On the other hand, the number of iterations roughly doubles as the number of subdomains doubles. The Neumann-Neumann preconditioner shows similar dependence on the number of subdomains. Additionally, its performance is negatively affected by an increasing number of grid points.

	Robin–Robin				Neumann–Neumann			
SDs \ Elems	1642	3352	8319	32814	1642	3352	8319	32814
2	32	34	52	30	34	73	152	117
4	48	74	94	91	77	176	403	> 1000
8	70	157	136	178	89	360	999	> 1000
16	278	358	171	288	359	509	951	> 1000
32	498	674	679	461	595	865	> 1000	> 1000
System Size $\approx$	3000	6000	13500	51000	3000	6000	13500	51000

Table 5.5. Influence of the number of subdomains and elements on the number of sQMR iterations; $\alpha = 10^{-5}$, $\varepsilon = 5 \times 10^{-4}$.

Finally, we rerun all tests from the third experiment using GMRES instead of sQMR. Detailed results are presented in Table 5.6. We observe that GMRES requires fewer iterations than sQMR. It appears that the dependence on the number of subdomains for the

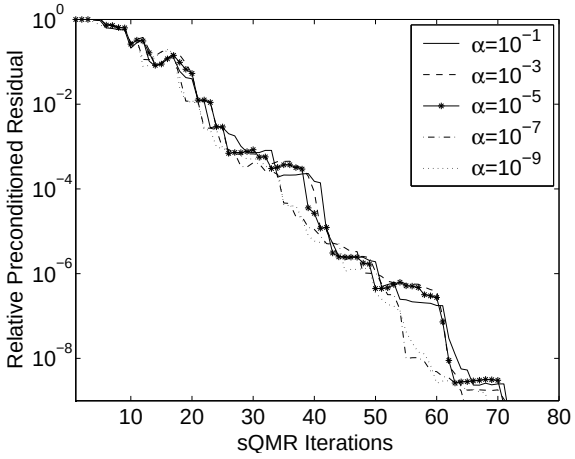

Figure 5.5. Influence of the regularization α on the R–R prec., for a fixed diffusion $\varepsilon = 5 \times 10^{-4}$.

Robin–Robin preconditioner is not nearly as pronounced as in the sQMR case. On the other hand, its mesh independence is clearly confirmed in the GMRES experiment. The Neumann-Neumann preconditioner performs better than in the sQMR runs, however, it remains dependent both on the number of subdomains and the mesh size.

	Robin–Robin				Neumann–Neumann			
SDs \ Elems	1642	3352	8319	32814	1642	3352	8319	32814
2	20	28	40	20	21	34	46	42
4	29	43	61	41	37	56	85	80
8	35	64	73	70	42	78	117	151
16	76	81	70	75	84	100	131	204
32	117	116	115	95	134	157	244	245
System Size $\approx$	3000	6000	13500	51000	3000	6000	13500	51000

Table 5.6. Influence of the number of subdomains and elements on the number of GMRES iterations; $\alpha = 10^{-5}$, $\varepsilon = 5 \times 10^{-4}$.

5.3 Robin Boundary Control

The domain decomposition method described in the previous section for optimal control problems with distributed control can be extended to problems with boundary control using the ideas in [20]. We report on some numerical results for the example problem

$$\text{minimize } \frac{1}{2}\int_{\Omega}(y(x)-\widehat{y}(x))^2dx+\frac{\alpha}{2}\int_{\partial\Omega_c}u^2(x)dx \tag{5.5a}$$

subject to

$$-\varepsilon\Delta y(x)+\mathbf{a}(x)\cdot\nabla y(x)+r(x)y(x)=f(x), \qquad x\in\Omega, \tag{5.5b}$$

$$y(x)=0, \qquad x\in\partial\Omega_D, \tag{5.5c}$$

$$\varepsilon\frac{\partial}{\partial\mathbf{n}}y(x)+\delta y(x)=\delta u(x), \qquad x\in\partial\Omega_c \tag{5.5d}$$

where $r=1$, $f=0$, and $\delta=10^3$. The Robin boundary condition (5.5d) can be viewed as a penalized Dirichlet condition [6, 21].

The first experiment is set up as in Example 5.1.1. We examine the performance of the Robin–Robin and Neumann-Neumann preconditioners with respect to various velocity fields, on the rectangular domain $\Omega=(0,1)\times(0,0.2)$ with five square subdomains. We choose $\partial\Omega_c=\partial\Omega$, i.e. $\partial\Omega_D=\emptyset$. In Tables 5.7 and 5.8 we report the number of preconditioned sQMR iterations for the values $\alpha=10^{-4}$ and $\alpha=1$, respectively.

ε	Prec. \ Velocity	Normal	Parallel	Oblique	Rotating
0.001	R-R	16	3	9	9
	N-N	129	3	36	17
1	R-R	4	4	4	4
	N-N	4	4	4	4

Table 5.7. sQMR iterations for different velocity fields and fixed regularization parameter $\alpha=10^{-4}$.

The obtained results are similar to those of Example 5.1.1, with one important difference. For small ε, the Neumann-Neumann preconditioner performs significantly worse when compared to the distributed control case. This behavior can be explained by re-examining Remark 4.3. The boundary control problem lacks the property $\text{rank}(\mathbf{B}^i)=\mathbb{R}^{m^i}$. Therefore, the invertibility of $\mathbf{A}^i$ is now needed to ensure the invertibility of $\mathbf{K}^i$. Within the Neumann-Neumann preconditioner (i.e., no modification of the local bilinear form a_i), we have observed severely ill-conditioned $\mathbf{K}^i$'s in some subdomains (with estimated condition numbers of 10^6).

ε	Prec. \ Velocity	Normal	Parallel	Oblique	Rotating
0.001	R-R	7	3	3	6
	N-N	73	3	29	15
1	R-R	4	4	4	4
	N-N	4	4	4	4

Table 5.8. sQMR iterations for different velocity fields and fixed regularization parameter $\alpha = 1$.

The second experiment assesses the sensitivity of the Robin–Robin and Neumann–Neumann preconditioners to increases in the number of subdomains. We use the same setup as in Example 5.1.2, i.e. the square domain $\Omega = (0,1) \times (0,1)$ with various partitioning schemes. As before, the velocity is $\mathbf{a}(x) = 3\mathbf{e}_1$ and $\varepsilon = 0.001$. The results are presented in Table 5.9.

Reg.	Prec. \ Part.	4×1	8×1	16×1	1×16
$\alpha = 10^{-4}$	R-R	17	37	78	4
	N-N	> 500	> 500	> 500	4
$\alpha = 1$	R-R	7	14	28	3
	N-N	142	218	340	3

Reg.	Prec. \ Part.	2×2	4×4	8×8	16×16
$\alpha = 10^{-4}$	R-R	9	20	42	82
	N-N	151	> 500	> 500	> 500
$\alpha = 1$	R-R	5	11	19	36
	N-N	83	163	260	420

Table 5.9. sQMR iterations for varying numbers of subdomains and fixed diffusivity $\varepsilon = 0.001$.

There are several major differences compared to the distributed control case. For the Robin–Robin preconditioner, the number of sQMR iterations roughly doubles as the number of subdomains in the x_1-direction doubles, regardless of the size of the regularization parameter α (i.e. small α does not yield partition independence). The failure of the Neumann-Neumann preconditioning scheme is evident. The preconditioned sQMR algorithm fails to achieve the desired relative residual within 500 iterations for six test cases. This result reinforces our conjecture from the previous experiment. When the regularization parameter is increased from $\alpha = 10^{-4}$ to $\alpha = 1$, the number of Robin–Robin preconditioned sQMR iterations is roughly reduced by a factor of two for all test cases. This result is more intuitive than the one in the distributed control example.

The third experiment examines the influence of the number of grid points. The problem is set up as in Example 5.1.2, where we fix two particular subdomain partitions (8×1 and 4×4), and vary the grid size. The results are presented in Table 5.10.

		8×1 Partition		
Reg.	Prec. \ Grid Size	32×32	64×64	128×128
$\alpha = 10^{-4}$	R-R	38	36	37
	N-N	> 500	> 500	> 500
$\alpha = 1$	R-R	14	14	14
	N-N	224	219	220

		4×4 Partition		
Reg.	Prec. \ Grid Size	32×32	64×64	128×128
$\alpha = 10^{-4}$	R-R	21	20	20
	N-N	> 500	> 500	> 500
$\alpha = 1$	R-R	12	12	11
	N-N	147	167	158

Table 5.10. sQMR iterations for varying numbers of grid points and fixed diffusivity $\varepsilon = 0.001$.

The results indicate that the convergence of the sQMR algorithm with the Robin–Robin preconditioner is mesh independent. This agrees with the observations made in the distributed control case. It is difficult to draw any conclusions about the performance of the Neumann-Neumann preconditioner as a function of the increasing number of grid points, since it performs quite poorly even for large α, and entirely fails to reach the desired relative residual for small α.

5.4 Solid/Fluid Temperature Control

Our last example is a simple solid/fluid temperature control problem motivated by [17]. The domain $\Omega = (0,1)^2$ is split into the subdomain $\Omega_f = (0,1) \times (0,0.75)$ occupied by a fluid, and the subdomain $\Omega_s = (0,1) \times (0.75,1)$ occupied by a solid. All length measurements are in meters. The velocity of the fluid is assumed to be $\mathbf{a}(x) = (1.5x_2 - 2x_2^2, 0)^T$ [m/sec]. We want to control the temperature y at the inflow boundary $\partial\Omega_c = \{0\} \times (0,0.75)$ to achieve a uniform temperature profile inside the solid. The boundary control problem is given by

$$\text{minimize } \frac{1}{2}\int_{\Omega_s} (y(x) - \widehat{y}(x))^2 dx + \frac{\alpha}{2}\int_{\partial\Omega_c} u^2(x) dx \tag{5.6a}$$

subject to

$$-\varepsilon_f \Delta y(x) + \mathbf{a}(x) \cdot \nabla y(x) = 0, \qquad x \in \Omega_f, \tag{5.6b}$$

$$-\varepsilon_s \Delta y(x) = f, \qquad x \in \Omega_s, \tag{5.6c}$$

$$\varepsilon \frac{\partial}{\partial \mathbf{n}} y(x) = 0, \qquad x \in \partial\Omega \setminus \partial\Omega_c, \tag{5.6d}$$

$$y(x) = d(x) + u(x), \qquad x \in \partial\Omega_c, \tag{5.6e}$$

where $\varepsilon_f = 0.6\,[W/(\mathrm{m}^\circ\mathrm{C})]$ is the thermal conductivity of the fluid (water), $\varepsilon_s = 237\,[W/(\mathrm{m}^\circ\mathrm{C})]$ is the thermal conductivity of the solid (aluminum), ε stands for either ε_f or ε_s, $f = 1.2 \times 10^4\,[W/\mathrm{m}^3]$ is the volumetric heat energy added to the solid, $\widehat{y}(x) = 90\,[^\circ\mathrm{C}]$ is the desired temperature of the solid, $d(x) = 70\,[^\circ\mathrm{C}]$ is a constant temperature on the control boundary $\partial\Omega_c$ representing the inflow temperature of the fluid for the uncontrolled (forward) problem, and $\alpha = 10^{-4}$ is a regularization parameter.

Figure 5.6 depicts the problem geometry along with the described velocity field. The domain is partitioned into $4 \times 4, \ldots, 32 \times 32$ equal sized subdomains such that each subdomain is either a subset of the fluid or the solid region. The weighting $\mathbf{D}_i$ in our preconditioner is not modified to account for the different thermal conductivities. This could be easily done following [13]. However, the reported iteration numbers below are not significantly different from those observed when $\varepsilon_f = \varepsilon_s = 1$ and therefore a modification of $\mathbf{D}_i$ has not been pursued in this example.

The presence of Dirichlet boundary controls requires a few changes in the discretization of the problem and its decomposition. These will be sketched in the following subsection.

5.4.1 Problem Discretization and Decomposition

We discretize (5.6) using conforming linear finite elements. Let $\{T_l\}$ be a triangulation of Ω. The state y is approximated using piecewise linear functions. The discretized state space is

$$Y^h = \left\{ \phi_h \in H^1(\Omega) \,:\, \phi_h|_{T_l} \in P^1(T_l) \text{ for all } l \right\}.$$

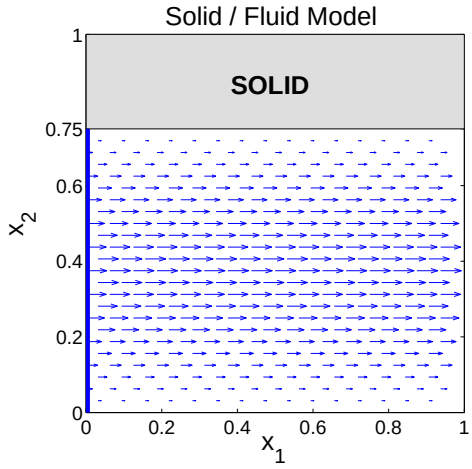

Figure 5.6. Velocity field and the control boundary (bold vertical line).

For the Dirichlet boundary control problem (5.6) the control space is $U = H^1(\partial\Omega_c)$ [17] and not $U = L^2(\partial\Omega_c)$ (as in the case of Robin boundary controls). Our controls are now discretized using piecewise linear functions which are continuous on $\partial\Omega_c$. The space of discretized controls is

$$U^h = \left\{ \mu_h \in H^1(\partial\Omega_c) \,:\, \mu_h|_{\partial T_l \cap \partial\Omega_c} \in P^1(\partial T_l \cap \partial\Omega_c) \text{ for all } l \right\}.$$

To simplify the presentation of the discretized problem, we assume that the vertices $x_1, \ldots, x_m$ of the triangulation are ordered such that the first n vertices lie on the controlled boundary $\partial\Omega_c$. Let $\phi_1, \ldots, \phi_m$ be the piecewise linear nodal basis for Y^h and let $\mu_1, \ldots, \mu_n$ be the piecewise linear nodal basis for U^h. In the following δ_{jk} denotes the Kronecker delta. If we define

$$\mathbf{A}_{jk} = a_h(\phi_k, \phi_j), \quad \mathbf{b}_j = \langle f, \phi_j \rangle_h, \quad j = n+1, \ldots, m, \quad k = 1, \ldots, m,$$

$$\mathbf{A}_{jk} = \delta_{jk}, \quad \mathbf{b}_j = 0, \quad j = 1, \ldots, n, \quad k = 1, \ldots, m,$$

$$\mathbf{B}_{jk} = \delta_{jk}, j = 1, \ldots, m, \quad k = 1, \ldots, n,$$

$\mathbf{Q}_{jk} = \langle \phi_k, \phi_j \rangle$, $j,k = 1, \ldots, m$, $\mathbf{c}_j = -\langle \hat{y}, \phi_j \rangle$, $j = 1, \ldots, m$, and $\mathbf{R}_{jk} = \langle \mu_k, \mu_j \rangle_{L^2(\partial\Omega_c)} + \langle \mu_k', \mu_j' \rangle_{L^2(\partial\Omega_c)}$, then our discretization of (5.6) is given by (4.1).

To decompose the problem, we again divide Ω into nonoverlapping subdomains Ω_i, $i = 1, \ldots, s$, such that each T_l belongs to exactly one $\overline{\Omega}_i$. We define Γ_i to be the interface between Ω_i and the other subdomains,

$$\Gamma_i = \partial\Omega_i \cap (\cup_{j \neq i} \partial\Omega_j),$$

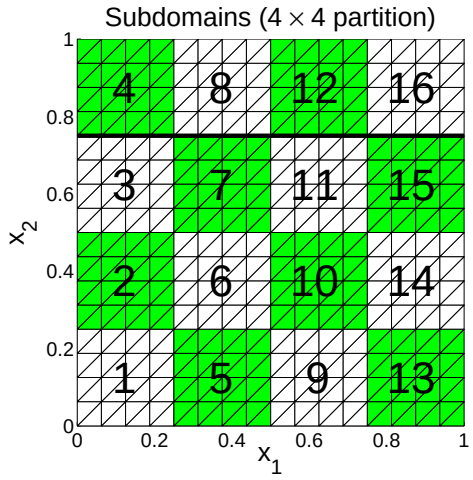

Figure 5.7. Decomposition of Ω into 4×4 subdomains.

and $\Gamma = \cup_{i=1}^{s} \Gamma_i$. As before, the unit outward normal of Ω_i is denoted by $\mathbf{n}_i$. A sample decomposition into 4×4 subdomains is shown in Figure 5.7.

The state space Y^h is is decomposed into $Y^h = Y^h_\Gamma \cup (\cup_{i=1}^{s} Y^h_{i,0})$, where

$$\begin{aligned} Y^h_i &= \left\{ \phi_h \in H^1(\Omega_i) \,:\, \phi_h|_{T_l} \in P^1(T_l) \text{ for all } T_l \subset \overline{\Omega}_i \right\}, && i = 1, \ldots, s, \\ Y^h_{i,0} &= \left\{ \phi_h \in Y^h_i \,:\, \phi_h = 0 \text{ on } \Gamma_i \right\}, && i = 1, \ldots, s, \\ Y^h_{i,\Gamma_i} &= Y^h_i \setminus Y^h_{i,0}, && i = 1, \ldots, s, \end{aligned}$$

and

$$Y^h_\Gamma = Y^h \setminus \left(\cup_{i=1}^{s} Y^h_{i,0} \right),$$

where in the latter case, $Y^h_{i,0}$ is viewed as a subspace of Y^h by extending $v_i \in Y^h_{i,0}$ by zero onto Ω. We split the space of discretized controls $U^h = U^h_\Gamma \cup (\cup_{i=1}^{s} U^h_{i,0})$, where

$$\begin{aligned} U^h_i &= \left\{ \mu_h \in H^1(\partial\Omega_i \cap \partial\Omega_c) \,:\, \mu_h|_{\partial T_l \cap \partial\Omega_c} \in P^1(\partial T_l \cap \partial\Omega_c) \text{ for all } T_l \subset \overline{\Omega}_i \right\}, && i = 1, \ldots, s, \\ U^h_{i,0} &= \left\{ \mu_h \in U^h_i \,:\, \mu_h = 0 \text{ on } \Gamma_i \right\}, && i = 1, \ldots, s, \\ U^h_{i,\Gamma_i} &= U^h_i \setminus U^h_{i,0}, && i = 1, \ldots, s, \end{aligned}$$

and $U^h_\Gamma = U^h \setminus \left(\cup_{i=1}^{s} U^h_{i,0} \right)$. Here $U^h_{i,0}$ is viewed as a subspace of U^h by extending $u_i \in U^h_{i,0}$ by zero onto $\partial\Omega_c$. Note that $U^h_i = \emptyset$ for subdomains Ω_i with $\partial\Omega_i \cap \partial\Omega_c = \emptyset$.

We split the subdomains into no-control subdomains

$$\mathcal{N} = \{ i \,:\, \partial\Omega_i \cap \partial\Omega_c = \emptyset \}$$

and control subdomains

$$\mathcal{C} = \{i : \partial\Omega_i \cap \partial\Omega_c \neq \emptyset\}.$$

For $i = 1, \ldots, s$, we define the submatrices $\mathbf{A}_{II}^i \in \mathbb{R}^{m_I^i \times m_I^i}$, $\mathbf{A}_{\Gamma I}^i \in \mathbb{R}^{m_\Gamma^i \times m_I^i}$, $\mathbf{A}_{I\Gamma}^i \in \mathbb{R}^{m_I^i \times m_\Gamma^i}$, and $\mathbf{A}_{\Gamma\Gamma}^i \in \mathbb{R}^{m_\Gamma^i \times m_\Gamma^i}$, where m_I^i is the number of nodes in $\overline{\Omega}_i \setminus \Gamma_i$ and m_Γ^i is the number of nodes in Γ_i, as follows. Let i_k be the global node number of the kth node in $\overline{\Omega}_i \setminus \Gamma_i$ and let γ_k be the global node number of the kth node in Γ_i. We set

$$\begin{aligned}
(\mathbf{A}_{II}^i)_{jk} &= a_{i,h}(\phi_{i_k}, \phi_{i_j}), && x_{i_j} \in \overline{\Omega}_i \setminus (\Gamma_i \cup \partial\Omega_c),\ x_{i_k} \in \overline{\Omega}_i \setminus \Gamma_i,\\
(\mathbf{A}_{I\Gamma}^i)_{jk} &= a_{i,h}(\phi_{\gamma_k}, \phi_{i_j}), && x_{i_j} \in \overline{\Omega}_i \setminus (\Gamma_i \cup \partial\Omega_c),\ x_{\gamma_k} \in \Gamma_i,\\
(\mathbf{A}_{\Gamma I}^i)_{jk} &= a_{i,h}(\phi_{i_k}, \phi_{\gamma_j}), && x_{\gamma_j} \in \Gamma_i \setminus \partial\Omega_c,\ x_{i_k} \in \overline{\Omega}_i \setminus \Gamma_i,\\
(\mathbf{A}_{\Gamma\Gamma}^i)_{jk} &= a_{i,h}(\phi_{\gamma_k}, \phi_{\gamma_j}), && x_{\gamma_j} \in \Gamma_i \setminus \partial\Omega_c,\ x_{\gamma_k} \in \Gamma_i,\\
(\mathbf{A}_{II}^i)_{jk} &= \delta_{jk}, && x_{i_j} \in (\overline{\Omega}_i \cap \partial\Omega_c) \setminus \Gamma_i,\ x_{i_k} \in \overline{\Omega}_i \setminus \Gamma_i,\\
(\mathbf{A}_{I\Gamma}^i)_{jk} &= 0, && x_{i_j} \in (\overline{\Omega}_i \cap \partial\Omega_c) \setminus \Gamma_i,\ x_{\gamma_k} \in \Gamma_i,\\
(\mathbf{A}_{\Gamma I}^i)_{jk} &= 0, && x_{\gamma_j} \in \Gamma_i \cap \partial\Omega_c,\ x_{i_k} \in \overline{\Omega}_i \setminus \Gamma_i,\\
(\mathbf{A}_{\Gamma\Gamma}^i)_{jk} &= \tfrac{1}{2}\delta_{jk}, && x_{\gamma_j} \in \Gamma_i \cap \partial\Omega_c \cap_{l\neq i} \Gamma_l,\ x_{\gamma_k} \in \Gamma_i,\\
(\mathbf{A}_{\Gamma\Gamma}^i)_{jk} &= \delta_{jk}, && x_{\gamma_j} \in (\Gamma_i \cap \partial\Omega_c) \setminus (\cap_{l\neq i}\Gamma_l),\ x_{\gamma_k} \in \Gamma_i.
\end{aligned}$$

The $\frac{1}{2}\delta_{jk}$ is used because in our problem set-up each point $x_{\gamma_j} \in \Gamma_i \cap \partial\Omega_c \cap_{l\neq i} \Gamma_l$ is shared by two subdomains. Moreover, we set $\mathbf{A}_{\Gamma\Gamma} = \sum_{i=1}^s (\mathbb{I}_i^y)^T \mathbf{A}_{\Gamma\Gamma}^i \mathbb{I}_i^y$, where $\mathbb{I}_i^y$ is the restriction operator which maps from the vector of coefficient unknowns on the interface boundary Γ, to only those associated with the interface boundary Γ_i of the ith subdomain. As before, after a suitable reordering of rows and columns, the stiffness matrix can be written as (4.4). The vector $\mathbf{b}$ is decomposed analogously to $\mathbf{A}$.

For $i = 1, \ldots, s$, we define the submatrices $\mathbf{Q}_{II}^i \in \mathbb{R}^{m_I^i \times m_I^i}$, $\mathbf{Q}_{\Gamma I}^i \in \mathbb{R}^{m_\Gamma^i \times m_I^i}$, and $\mathbf{Q}_{\Gamma\Gamma}^i \in \mathbb{R}^{m_\Gamma^i \times m_\Gamma^i}$, as follows.

$$\begin{aligned}
(\mathbf{Q}_{II}^i)_{jk} &= \langle \phi_{i_k}, \phi_{i_j} \rangle, && x_{i_j}, x_{i_k} \in \overline{\Omega}_i \setminus \Gamma_i,\\
(\mathbf{Q}_{I\Gamma}^i)_{jk} &= (\mathbf{Q}_{\Gamma I}^i)_{kj} = \langle \phi_{\gamma_k}, \phi_{i_j} \rangle, && x_{i_j} \in \overline{\Omega}_i \setminus \Gamma_i,\ x_{\gamma_k} \in \Gamma_i,\\
(\mathbf{Q}_{\Gamma\Gamma}^i)_{jk} &= \langle \phi_{\gamma_k}, \phi_{\gamma_j} \rangle, && x_{\gamma_j}, x_{\gamma_k} \in \Gamma_i
\end{aligned}$$

and $\mathbf{Q}_{\Gamma\Gamma} = \sum_{i=1}^s (\mathbb{I}_i^y)^T \mathbf{Q}_{\Gamma\Gamma}^i \mathbb{I}_i^y$. With this decomposition, $\mathbf{Q}$ can be written in the form (4.4). The vector $\mathbf{c}$ is decomposed analogously to $\mathbf{Q}$.

The matrices $\mathbf{B}, \mathbf{R}$ associated with the controls are decomposed as follows. For $i \in \mathcal{C}$, we define the submatrices $\mathbf{B}_{II}^i \in \mathbb{R}^{n_I^i \times m_I^i}$, $\mathbf{B}_{\Gamma I}^i \in \mathbb{R}^{n_\Gamma^i \times m_I^i}$, and $\mathbf{B}_{\Gamma\Gamma}^i \in \mathbb{R}^{n_\Gamma^i \times m_\Gamma^i}$, where n_I^i is the number of nodes in $(\partial\Omega_i \cap \partial\Omega_c) \setminus \Gamma_i$ and n_Γ^i is the number of nodes in $\Gamma_i \cap \partial\Omega_c$, as follows. As before, we let i_k be the global node number of the kth node in $\overline{\Omega}_i \setminus \Gamma_i$ and let γ_k be the global node number of the kth node in Γ_i. To simplify our presentation we assume that the first n_I^i nodes with global index $i_1, \ldots, i_{n_I^i}$ lie on the controlled boundary $(\partial\Omega_i \cap \partial\Omega_c) \setminus \Gamma_i$ and

that the first n_Γ^i nodes with global index $\gamma_1,\dots,\gamma_{n_\Gamma^i}$ lie on the controlled boundary $\Gamma_i\cap\partial\Omega_a$. We set

$$\begin{aligned}
(\mathbf{B}_{II}^i)_{jk} &= 0, && x_{i_j}\in\overline{\Omega}_i\setminus(\Gamma_i\cup\partial\Omega_c),\ x_{i_k}\in(\partial\Omega_i\cap\partial\Omega_c)\setminus\Gamma_i,\\
(\mathbf{B}_{I\Gamma}^i)_{jk} &= 0, && x_{i_j}\in\overline{\Omega}_i\setminus(\Gamma_i\cup\partial\Omega_c),\ x_{\gamma_k}\in\Gamma_i\cap\partial\Omega_c,\\
(\mathbf{B}_{\Gamma I}^i)_{jk} &= 0, && x_{\gamma_j}\in\Gamma_i\setminus\partial\Omega_c,\ x_{i_k}\in(\partial\Omega_i\cap\partial\Omega_c)\setminus\Gamma_i,\\
(\mathbf{B}_{\Gamma\Gamma}^i)_{jk} &= 0, && x_{\gamma_j}\in\Gamma_i\setminus\partial\Omega_c,\ x_{\gamma_k}\in\Gamma_i\cap\partial\Omega_c,\\
(\mathbf{B}_{II}^i)_{jk} &= \delta_{jk}, && x_{i_j}\in(\overline{\Omega}_i\cap\partial\Omega_c)\setminus\Gamma_i,\ x_{i_k}\in(\partial\Omega_i\cap\partial\Omega_c)\setminus\Gamma_i,\\
(\mathbf{B}_{I\Gamma}^i)_{jk} &= 0, && x_{i_j}\in(\overline{\Omega}_i\cap\partial\Omega_c)\setminus\Gamma_i,\ x_{\gamma_k}\in\Gamma_i\cap\partial\Omega_c,\\
(\mathbf{B}_{\Gamma I}^i)_{jk} &= 0, && x_{\gamma_j}\in\Gamma_i\cap\partial\Omega_c,\ x_{i_k}\in(\partial\Omega_i\cap\partial\Omega_c)\setminus\Gamma_i,\\
(\mathbf{B}_{\Gamma\Gamma}^i)_{jk} &= \tfrac{1}{2}\delta_{jk}, && x_{\gamma_j}\in\Gamma_i\cap\partial\Omega_c\cap_{l\neq i}\Gamma_l,\ x_{\gamma_k}\in\Gamma_i\cap\partial\Omega_c,\\
(\mathbf{B}_{\Gamma\Gamma}^i)_{jk} &= \delta_{jk}, && x_{\gamma_j}\in(\Gamma_i\cap\partial\Omega_c)\setminus(\cap_{l\neq i}\Gamma_l),\ x_{\gamma_k}\in\Gamma_i\cap\partial\Omega_c.
\end{aligned}$$

Moreover, we set $\mathbf{B}_{\Gamma\Gamma}=\sum_{i=1}^s(\mathbb{I}_i^u)^T\mathbf{B}_{\Gamma\Gamma}^i\mathbb{I}_i^u$, where $\mathbb{I}_i^u$ is the restriction operator which maps from the vector of coefficient unknowns on the interface control boundary $\Gamma\cap\partial\Omega_c$, to only those associated with the interface control boundary $\Gamma_i\cap\partial\Omega_c$ of the ith subdomain.

For $i\in\mathcal{C}$, we define the submatrices $\mathbf{R}_{II}^i\in\mathbb{R}^{n_I^i\times n_I^i}$, $\mathbf{R}_{\Gamma I}^i=(\mathbf{R}_{I\Gamma}^i)^T\in\mathbb{R}^{n_\Gamma^i\times n_I^i}$, and $\mathbf{R}_{\Gamma\Gamma}^i\in\mathbb{R}^{n_\Gamma^i\times n_\Gamma^i}$ with

$$\begin{aligned}
(\mathbf{R}_{II}^i)_{jk} &= \langle\mu_{i_k},\mu_{i_j}\rangle_{L^2(\partial\Omega_i\cap\partial\Omega_c)}+\langle\mu'_{i_k},\mu'_{i_j}\rangle_{L^2(\partial\Omega_i\cap\partial\Omega_c)}, && x_{i_j},x_{i_k}\in(\partial\Omega_i\cap\partial\Omega_c)\setminus\Gamma_i,\\
(\mathbf{R}_{I\Gamma}^i)_{jk} &= \langle\mu_{\gamma_k},\mu_{i_j}\rangle_{L^2(\partial\Omega_i\cap\partial\Omega_c)}+\langle\mu'_{\gamma_k},\mu'_{i_j}\rangle_{L^2(\partial\Omega_i\cap\partial\Omega_c)}, && x_{i_j}\in(\partial\Omega_i\cap\partial\Omega_c)\setminus\Gamma_i,\ x_{\gamma_k}\in\Gamma_i\cap\partial\Omega_c,\\
(\mathbf{R}_{\Gamma\Gamma}^i)_{jk} &= \langle\mu_{\gamma_k},\mu_{\gamma_j}\rangle_{L^2(\partial\Omega_i\cap\partial\Omega_c)}+\langle\mu'_{\gamma_k},\mu'_{\gamma_j}\rangle_{L^2(\partial\Omega_i\cap\partial\Omega_c)}, && x_{\gamma_j},x_{\gamma_k}\in\Gamma_i\cap\partial\Omega_c
\end{aligned}$$

and $\mathbf{R}_{\Gamma\Gamma}=\sum_{i=1}^s(\mathbb{I}_i^u)^T\mathbf{R}_{\Gamma\Gamma}^i\mathbb{I}_i^u$. With this decomposition, $\mathbf{R}$ can be written in the form (4.4).

We can now insert the domain decomposition structure of the matrices $\mathbf{A},\mathbf{Q},\mathbf{B},\mathbf{R}$ into the system of optimality conditions (4.2) for our discretization of (5.6) and perform a symmetric permutation. We obtain

$$\begin{pmatrix}\mathbf{K}_{II}^1 & & & (\mathbf{K}_{\Gamma I}^1)^T\\ & \ddots & & \vdots\\ & & \mathbf{K}_{II}^s & (\mathbf{K}_{\Gamma I}^s)^T\\ \mathbf{K}_{\Gamma I}^1 & \cdots & \mathbf{K}_{\Gamma I}^s & \mathbf{K}_{\Gamma\Gamma}\end{pmatrix}\begin{pmatrix}\mathbf{x}_I^1\\ \vdots\\ \mathbf{x}_I^d\\ \mathbf{x}_\Gamma\end{pmatrix}=\begin{pmatrix}\mathbf{g}_I^1\\ \vdots\\ \mathbf{g}_I^d\\ \mathbf{g}_\Gamma\end{pmatrix},$$

where

$$\mathbf{K}_{\Gamma\Gamma}^i=\begin{pmatrix}\mathbf{Q}_{\Gamma\Gamma}^i & & (\mathbf{A}_{\Gamma\Gamma}^i)^T\\ & \alpha\mathbf{R}_{\Gamma\Gamma}^i & (\mathbf{B}_{\Gamma\Gamma}^i)^T\\ \mathbf{A}_{\Gamma\Gamma}^i & \mathbf{B}_{\Gamma\Gamma}^i & \end{pmatrix},i=1,\dots,s,\quad \mathbf{K}_{\Gamma\Gamma}=\sum_{i=1}^s\mathbf{K}_{\Gamma\Gamma}^i,$$

$$\mathbf{K}_{II}^i=\begin{pmatrix}\mathbf{Q}_{II}^i & & (\mathbf{A}_{II}^i)^T\\ & \alpha\mathbf{R}_{II}^i & (\mathbf{B}_{II}^i)^T\\ \mathbf{A}_{II}^i & \mathbf{B}_{II}^i & \end{pmatrix},\quad \mathbf{K}_{\Gamma I}^i=\begin{pmatrix}\mathbf{Q}_{\Gamma I}^i & & (\mathbf{A}_{I\Gamma}^i)^T\\ & \alpha\mathbf{R}_{\Gamma I}^i & (\mathbf{B}_{I\Gamma}^i)^T\\ \mathbf{A}_{\Gamma I}^i & \mathbf{B}_{\Gamma I}^i & \end{pmatrix},\quad i\in\mathcal{C}$$

and

$$\mathbf{K}_{II}^i = \begin{pmatrix} \mathbf{Q}_{II}^i & (\mathbf{A}_{II}^i)^T \\ \mathbf{A}_{II}^i & \end{pmatrix}, \quad \mathbf{K}_{\Gamma I}^i = \begin{pmatrix} \mathbf{Q}_{\Gamma I}^i & (\mathbf{A}_{I\Gamma}^i)^T \\ \mathbf{A}_{\Gamma I}^i & \end{pmatrix}, \quad i \in \mathcal{N}.$$

Furthermore,

$$\mathbf{x}_\Gamma = \begin{pmatrix} \mathbf{y}_\Gamma \\ \mathbf{u}_\Gamma \\ \mathbf{p}_\Gamma \end{pmatrix}, \mathbf{g}_\Gamma = \begin{pmatrix} -\mathbf{c}_\Gamma \\ \mathbf{0} \\ \mathbf{b}_\Gamma \end{pmatrix},$$

and

$$\mathbf{x}_I^i = \begin{pmatrix} \mathbf{y}_I^i \\ \mathbf{u}_I^i \\ \mathbf{p}_I^i \end{pmatrix}, \mathbf{g}_I^i = \begin{pmatrix} -\mathbf{c}_I^i \\ \mathbf{0} \\ \mathbf{b}_I^i \end{pmatrix}, i \in \mathcal{C}, \quad \mathbf{x}_I^i = \begin{pmatrix} \mathbf{y}_I^i \\ \mathbf{p}_I^i \end{pmatrix}, \mathbf{g}_I^i = \begin{pmatrix} \mathbf{c}_I^i \\ \mathbf{b}_I^i \end{pmatrix}, i \in \mathcal{N}.$$

For subdomains Ω_i with $i \in \mathcal{N}$ the operator equation $\mathcal{S}_i(y_\Gamma, p_\Gamma) = r_i$ now corresponds to (cf. Theorem 3.4 and Remark 3.5)

$$-\varepsilon\Delta y_i(x) + \mathbf{a}(x)\cdot\nabla y_i(x) = f(x) \qquad \text{in } \Omega_i, \tag{5.7a}$$

$$\varepsilon\frac{\partial}{\partial \mathbf{n}_i} y_i(x) = 0, \qquad \text{on } \partial\Omega_i \cap \partial\Omega, \tag{5.7b}$$

$$\left(\varepsilon\frac{\partial}{\partial \mathbf{n}_i} - \tfrac{1}{2}\mathbf{a}(x)\cdot\mathbf{n}_i\right) y_i(x) = r_i^y(x) \qquad \text{on } \Gamma_i, \tag{5.7c}$$

$$-\varepsilon\Delta p_i(x) - \mathbf{a}(x)\cdot\nabla p_i(x) = -(y_i(x) - \hat{y}(x)) \qquad \text{in } \Omega_i, \tag{5.7d}$$

$$\varepsilon\frac{\partial}{\partial \mathbf{n}_i} p_i(x) + \mathbf{a}(x)\cdot\mathbf{n}(x)\; p_i(x) = 0, \qquad \text{on } \partial\Omega_i \cap \partial\Omega, \tag{5.7e}$$

$$\left(\varepsilon\frac{\partial}{\partial \mathbf{n}_i} + \tfrac{1}{2}\mathbf{a}(x)\cdot\mathbf{n}_i\right) p_i(x) = r_i^p(x) \qquad \text{on } \Gamma_i, \tag{5.7f}$$

with $\varepsilon = \varepsilon_s$, $\mathbf{a} = 0$ if $\Omega_i \subset \Omega_s$ and $\varepsilon = \varepsilon_f$, $f = 0$ if $\Omega_i \subset \Omega_f$. Note that in our example $r = 0$ and $\nabla\cdot\mathbf{a} = 0$. The bilinear forms $a_i(y_h, \phi_h)$ (cf. (3.9)) corresponding to these advection problems only satisfy $a_i(y,y) \geq c|y|^2_{1,\Omega_i}$ and the weak forms corresponding to (5.7) are not uniquely solvable. This is the same issue that arises in Neumann-Neumann preconditioners for the Laplace equation [10, 38, 39] and boundary control problems governed by the Laplace equation [20]. Motivated by these works, we consider the perturbations

$$-\varepsilon\Delta y_i(x) + \mathbf{a}(x)\cdot\nabla y_i(x) + \frac{\varepsilon}{H^2} y_i(x) = f(x) \qquad \text{in } \Omega_i, \tag{5.8a}$$

$$\varepsilon\frac{\partial}{\partial \mathbf{n}_i} y_i(x) = 0, \qquad \text{on } \partial\Omega_i \cap \partial\Omega, \tag{5.8b}$$

$$\left(\varepsilon\frac{\partial}{\partial \mathbf{n}_i} - \tfrac{1}{2}\mathbf{a}(x)\cdot\mathbf{n}_i\right) y_i(x) = r_i^y(x) \qquad \text{on } \Gamma_i, \tag{5.8c}$$

$$-\varepsilon\Delta p_i(x) - \mathbf{a}(x)\cdot\nabla p_i(x) + \frac{\varepsilon}{H^2} p_i(x) = -(y_i(x) - \hat{y}(x)) \qquad \text{in } \Omega_i, \tag{5.8d}$$

$$\varepsilon\frac{\partial}{\partial \mathbf{n}_i} p_i(x) + \mathbf{a}(x)\cdot\mathbf{n}(x)\; p_i(x) = 0, \qquad \text{on } \partial\Omega_i \cap \partial\Omega, \tag{5.8e}$$

$$\left(\varepsilon\frac{\partial}{\partial \mathbf{n}_i} + \tfrac{1}{2}\mathbf{a}(x)\cdot\mathbf{n}_i\right) p_i(x) = r_i^p(x) \qquad \text{on } \Gamma_i, \tag{5.8f}$$

where H is the lengths of the subdomain. This leads to subdomain Schur complement matrices $\widetilde{\mathbf{S}}_i^{-1}$. Our preconditioner is now given by

$$\mathbf{P} = \sum_i \mathbf{D}_i \mathbb{I}_i^T \widetilde{\mathbf{S}}_i^{-1} \mathbb{I}_i \mathbf{D}_i.$$

5.4.2 Numerical Results

Figure 5.8 shows a typical computed temperature profile for the controlled problem on a 64×64 grid with a 4×4 subdomain partition. The obtained boundary control is shown in Figure 5.9. We also include a side-by-side comparison of the temperature contour plots for the controlled problem and the uncontrolled problem, in which we ignore the control u and simply solve the forward problem (5.6b)-(5.6e), see Figures 5.10 and 5.11.

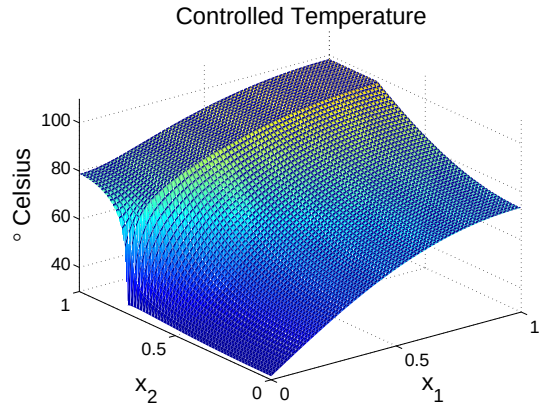

Figure 5.8. Computed temperature y for the controlled problem.

We now discuss two experiments that help us assess the efficiency of the Robin–Robin preconditioner. The first experiment examines the influence of the number of grid points on the performance of the GMRES algorithm with the Robin–Robin preconditioner. The results are presented in Table 5.11. They indicate that the number of GMRES iterations grows in nearly constant increments as the number of grid points is doubled in both x and y direction. Thus, for the solid/fluid control example, the performance of the Robin-Robin preconditioner is not mesh-independent.

In the second experiment, we examine the dependence on the number of subdomains. We focus on 4×4, 8×8, 16×16, and 32×32 subdomain partitions on a 128×128 grid. The results of Table 5.12 indicate that the number of GMRES iterations is proportional to the number of subdomains in the direction of the velocity field. This result agrees with the observations made in the previous example sections.

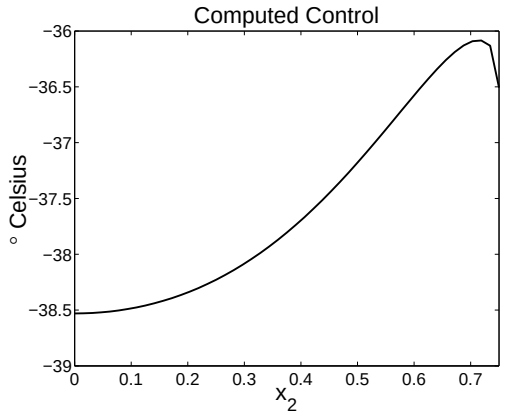

Figure 5.9. Computed boundary control u.

	4×4 Partition			
Grid Size	16×16	32×32	64×64	128×128
Iterations	58	77	94	109
	8×8 Partition			
Grid Size	16×16	32×32	64×64	128×128
Iterations	80	121	163	201

Table 5.11. GMRES iterations for varying numbers of grid points, solid/fluid example.

Partition	4×4	8×8	16×16	32×32
Iterations	109	201	325	487

Table 5.12. GMRES iterations for varying numbers of subdomains, solid/fluid example.

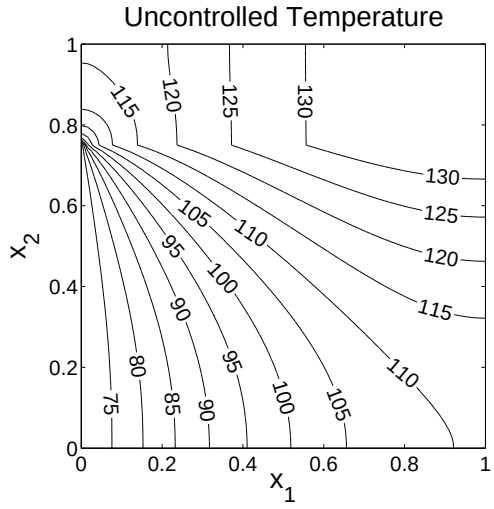

Figure 5.10. Contour plot of uncontrolled temperature (in °Celsius), as the solution of the forward problem with $d(x) = 70\,[^{\circ}\mathrm{C}]$.

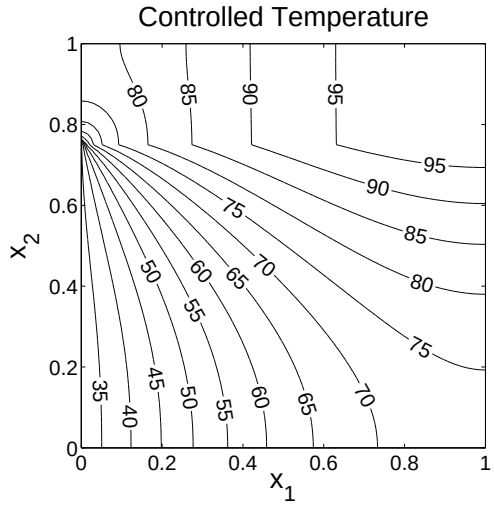

Figure 5.11. Contour plot of computed controlled temperature (in °Celsius).

6 Conclusions

We have introduced an optimization-level domain decomposition preconditioner for advection dominated linear-quadratic elliptic optimal control problems, which extends the work of [4, 3] to the optimization context.

The tasks required for the application of the domain decomposition preconditioner are closely related to what is required for the solution of the global optimal control problem, which allows code reuse and enables optimization-level parallelization of existing solvers for advection dominated linear-quadratic elliptic optimal control problems.

Numerical experiments have shown that the preconditioner is fairly insensitive to the velocity, the viscosity and the control regularization parameter. For distributed control and Robin boundary control test problems the preconditioner deteriorates only slowly as the number of subdomains increased.

Unfortunately, a theoretical explanation for the performance of the preconditioner is not yet available. Theoretical investigations, the application of the preconditioner to other problems, in particular 3D problems, and the design and incorporation of coarse spaces into the preconditioner are planned.

References

[1] F. Abraham, M. Behr, and M. Heinkenschloss. The effect of stabilization in finite element methods for the optimal boundary control of the Oseen equations. *Finite Elem. Anal. Des.*, 41:229–251, 2004.

[2] F. Abraham, M. Behr, and M. Heinkenschloss. Shape optimization in stationary blood flow: A numerical study of non-newtonian effects. *Computer Methods in Biomechanics and Biomedical Engineering*, 8:127–137, 2005.

[3] Y. Achdou and F. Nataf. A Robin-Robin preconditioner for an advection-diffusion problem. *C. R. Acad. Sci. Paris Sér. I Math.*, 325(11):1211–1216, 1997.

[4] Y. Achdou, P. Le Tallec, F. Nataf, and M. Vidrascu. A domain decomposition preconditioner for an advection-diffusion problem. *Comput. Methods Appl. Mech. Engrg.*, 184(2-4):145–170, 2000.

[5] V. Akçelik, G. Biros, O. Ghattas, K. R. Long, and B. van Bloemen Waanders. A variational finite element method for source inversion for convective-diffusive transport. *Finite Elem. Anal. Des.*, 39(8):683–705, 2003.

[6] I. Babuška. The finite element method with penalty. *Math. Comp.*, 27:221–228, 1973.

[7] A. N. Brooks and T. J. R. Hughes. Streamline upwind/Petrov–Galerkin formulations for convection dominated flows with particular emphasis on the incompressible Navier–Stokes equations. *Comp. Meth. Appl. Mech. Engng.*, 32:199–259, 1982.

[8] S. S. Collis and M. Heinkenschloss. Analysis of the streamline upwind/petrov galerkin method applied to the solution of optimal control problems. Technical Report TR02–01, Department of Computational and Applied Mathematics, Rice University, Houston, TX 77005–1892, 2002. http://www.caam.rice.edu/∼heinken.

[9] T. A. Davis. Algorithm 832: UMFPACK V4.3—an unsymmetric-pattern multifrontal method. *ACM Trans. Math. Software*, 30(2):196–199, 2004.

[10] M. Dryja, B. F. Smith, and O. B. Widlund. Schwarz analysis of iterative substructuring algorithms for elliptic problems in three dimensions. *SIAM J. Numer. Anal.*, 31(3):1662–1694, 1994.

[11] R. W. Freund and N. M. Nachtigal. A new Krylov-subspace method for symmetric indefinite linear systems. In W. F. Ames, editor, *Proceedings of the 14th IMACS World Congress on Computational and Applied Mathematics*, pages 1253–1256. IMACS, 1994.

[12] R. W. Freund and N. M. Nachtigal. Software for simplified Lanczos and QMR algorithms. *Applied Numerical Mathematics*, 19:319–341, 1995.

[13] L. Gerardo-Giorda, P. Le Tallec, and F. Nataf. A Robin-Robin preconditioner for advection-diffusion equations with discontinuous coefficients. *Comput. Methods Appl. Mech. Engrg.*, 193(9-11):745–764, 2004.

[14] N. I. M. Gould. On practical conditions for the existence and uniqueness of solutions to the general equality quadratic programming problem. *Math. Programming*, 32(1):90–99, 1985.

[15] M. D. Gunzburger. *Perspectives in Flow Control and Optimization*. SIAM, Philadelphia, 2003.

[16] M. D. Gunzburger, L. S. Hou, and T. P. Svobotny. Heating and cooling control of temperature distributions along boundaries of flow domains. *J. of Mathematical Systems, Estimation, and Control*, 3:147–172, 1993.

[17] M. D. Gunzburger and H. C. Lee. Analysis, approximation, and computation of a coupled solid/fluid temperature control problems. *Comput. Methods Appl. Mech. Engrg.*, 118:133–152, 1994.

[18] G. Haase, U. Langer, and A. Meyer. Domain decomposition preconditioners with inexact subdomain solvers. *J. of Num. Lin. Alg. with Appl.*, 1(1):27–42, 1992.

[19] M. Heinkenschloss and H. Nguyen. Balancing Neumann-Neumann methods for elliptic optimal control problems. In R. Kornhuber, R. H. W. Hoppe, J. Periaux, O. Pironneau, O. B. Widlund, and J. Xu, editors, *Domain Decomposition methods in Science*

and Engineering, Lecture Notes in Computational Science and Engineering, Vol. 40, pages 589–596, Heidelberg, 2004. Springer-Verlag.

[20] M. Heinkenschloss and H. Nguyen. Neumann-Neumann domain decomposition preconditioners for linear–quadratic elliptic optimal control problems. Technical Report TR04–01, Department of Computational and Applied Mathematics, Rice University, 2004.

[21] L. S. Hou and S. S. Ravindran. Numerical approximation of optimal control problems by a penalty method: error estimates and numerical results. *SIAM Journal of Scientific Computing*, 20:1753–1777, 1999.

[22] K. Ito and S. S. Ravindran. Optimal control of thermally convected fluid flows. *SIAM J. on Scientific Computing*, 19:1847–1869, 1998.

[23] G. Karypis. METIS. http://www-users.cs.umn.edu/∼karypis/metis.

[24] D. E. Keyes and W. D. Gropp. A comparison of domain decomposition techniques for elliptic partial differential equations and their parallel implementation. *SIAM J. Scientific and Statistical Computing*, 8:S166–S202, 1987.

[25] P. Knabner and L. Angermann. *Numerical Methods for Partial Differential Equations*. Texts in Applied Mathematics, Vol. 44. Springer–Verlag, Berlin, Heidelberg, New York, 2003.

[26] T. Knopp, G. Lube, R. Gritzki, and M. Rösler. Simulation of indoor air movement using stabilized finite element methods. In *Finite element methods (Jyväskylä, 2000)*, volume 15 of *GAKUTO Internat. Ser. Math. Sci. Appl.*, pages 109–117. Gakk ̄otosho, Tokyo, 2001.

[27] T. Knopp, G. Lube, R. Gritzki, and M. Rösler. Iterative substructuring methods for incompressible non-isothermal flows and its application to indoor air flow simulation. *Internat. J. Numer. Methods Fluids*, 40(12):1527–1538, 2002.

[28] J.-L. Lions. *Optimal Control of Systems Governed by Partial Differential Equations*. Springer Verlag, Berlin, Heidelberg, New York, 1971.

[29] Tamara K. Locke. Guide to preparing SAND reports. Technical report SAND98-0730, Sandia National Laboratories, Albuquerque, New Mexico 87185 and Livermore, California 94550, May 1998.

[30] K. W. Morton. *Numerical Solution of Convection–Diffusion Problems*. Chapman & Hall, London, Glasgow, New York, 1996.

[31] A. Quarteroni and A. Valli. *Numerical Approximation of Partial Differential Equations*. Springer, Berlin, Heidelberg, New York, 1994.

[32] A. Quarteroni and A. Valli. *Domain Decomposition Methods for Partial Differential Equations*. Oxford University Press, Oxford, 1999.

[33] Z. Ren and J. Stewart. Simulating air flow and temperature distribution inside buildings using a modified version of COMIS with sub-zonal divisions. *Energy and Buildings*, 35(3):257–271, 2003.

[34] H. G. Roos, M. Stynes, and L. Tobiska. *Numerical Methods for Singularly Perturbed Differential Equations*. Computational Mathematics, Vol. 24. Springer–Verlag, Berlin, 1996.

[35] Y. Saad and M. H. Schultz. GMRES a generalized minimal residual algorithm for solving nonsymmetric linear systems. *SIAM J. Sci. Stat. Comp.*, 7:856–869, 1986.

[36] A. G. Salinger, R. P. Pawlowski, J. N. Shadid, and B. G. van Bloemen Waanders. Computational analysis and optimization of a chemical vapor deposition reactor with large-scale computing. *Industrial and Engineering Chemistry Research*, 43(16):4612 – 4623, 2004.

[37] J. R. Shewchuk. Triangle: Engineering a 2D quality mesh generator and delaunay triangulator. In Ming C. Lin and Dinesh Manocha, editors, *Applied Computational Geometry: Towards Geometric Engineering*, volume 1148 of *Lecture Notes in Computer Science*, pages 203–222. Springer-Verlag, 1996. From the First ACM Workshop on Applied Computational Geometry.

[38] B. Smith, P. Bjørstad, and W. Gropp. *Domain Decomposition. Parallel Multilevel Methods for Elliptic Partial Differential Equations*. Cambridge University Press, Cambridge, London, New York, 1996.

[39] A. Toselli and O. Widlund. *Domain Decomposition Methods - Algorithms and Theory*. Computational Mathematics, Vol. 34. Springer–Verlag, Berlin, 2004.

[40] C. R. Vogel. *Computational Methods for Inverse Problems*. Frontiers in Applied Mathematics, Vol 24. SIAM, Philadelphia, 2002.

[41] G. Z. Yang and N. Zabaras. An adjoint method for the inverse design of solidification processes with natural convection. *International Journal for Numerical Methods in Engineering*, 42:1121–1144, 1998.

DISTRIBUTION:

1 George Biros
Department of Mechanical Engineering and Applied Mechanics
University of Pennsylvania
Philadelphia, PA 19104-6315

1 Omar Ghattas
Civil & Environmental Engineering
Carnegie Mellon University
Pittsburgh, Pennsylvania 15213

1 William D. Gropp
Mathematics and Computer Science Division
Argonne National Laboratory
9700 South Cass Avenue
Argonne, Illinois 60439

1 Max Gunzburger
School of Computational Science & Information Technology
400 Dirac Science Library
Florida State University
Tallahassee, FL 32306-4120

1 Matthias Heinkenschloss
Department of Computational and Applied Mathematics
MS-134
Rice University
6100 Main Street
Houston, TX 77005-1892

1 Ronald Hoppe
Department of Mathematics
University of Houston
Houston, TX 77204-3008

1 David Keyes
Department of Applied Physics and Applied Mathematics
200 S. W. Mudd Building
500 W. 120th Street
New York, NY 10027

1 Denis Ridzal
Department of Computational and Applied Mathematics
MS-134
Rice University
6100 Main Street
Houston, TX 77005-1892

1 Barry Smith
Mathematics and Computer Science Division
Argonne National Laboratory
9700 South Cass Avenue
Argonne, Illinois 60439

1 Olof Widlund
Courant Institute
251 Mercer Street
New York, New York 10012

1 M2497
Central Technical Files, 8945-1

1 MS 0370
Roscoe A. Bartlett, 9211

1 MS 0370
Bart G. van Bloemen Waanders, 9211

1 MS 0370
Scott A. Mitchell , 9211

1 MS 1110
David E. Womble, 9210

1 MS 1110
Scott S Collis, 9214

1 MS 1110
Mike A. Heroux , 9214

1 MS 1110
John N. Shadid, 9233

1 MS 1110
Andrew G. Salinger, 9233

2 MS 0899
Technical Library, 9616

1 MS 0612
Document Control Station, Attn:
Review & Approval Desk, 9612